



Universiteit
Leiden
The Netherlands

Cellular models for fundamental and applied biomedical research

Liu, J.

Citation

Liu, J. (2018, November 28). *Cellular models for fundamental and applied biomedical research*. Retrieved from <https://hdl.handle.net/1887/67296>

Version: Not Applicable (or Unknown)

License: [Licence agreement concerning inclusion of doctoral thesis in the Institutional Repository of the University of Leiden](#)

Downloaded from: <https://hdl.handle.net/1887/67296>

Note: To cite this publication please use the final published version (if applicable).

Cover Page



Universiteit Leiden



The handle <http://hdl.handle.net/1887/67296> holds various files of this Leiden University dissertation.

Author: Liu, J.

Title: Cellular models for fundamental and applied biomedical research

Issue Date: 2018-11-28

Chapter 4

Generation and primary characterization of iAM-1,
conditionally immortalized atrial myocytes with
preserved cardiomyogenic differentiation capacity

Liu J, Volkers L, Jangsangthong W, Bart CI, Engels MC, Zhou G, Schalijs MJ,
Ypey DL, Pijnappels DA, de Vries AAF

Adapted from: Cardiovasc Res. 2018. doi: 10.1093/cvr/cvy134.

Abstract

Aims: The generation of homogeneous cardiomyocyte populations from fresh tissue or stem cells is laborious and costly. A potential solution to this problem would be to establish lines of immortalized cardiomyocytes. However, as proliferation and (terminal) differentiation of cardiomyocytes are mutually exclusive processes, their permanent immortalization causes loss of electrical and mechanical functions. We therefore aimed at developing conditionally immortalized atrial myocyte (iAM) lines allowing toggling between proliferative and contractile phenotypes by a single-component change in culture medium composition.

Methods and results: Freshly isolated neonatal rat atrial cardiomyocytes (AMs) were transduced with a lentiviral vector conferring doxycycline-controlled expression of simian virus 40 large T antigen. Under proliferative conditions (*i.e.* in the presence of doxycycline), the resulting cells lost most cardiomyocyte traits and doubled every 38 hours. Under differentiation conditions (*i.e.* in the absence of doxycycline), the cells stopped dividing and spontaneously reacquired a phenotype very similar to that of primary AMs in gene expression profile, sarcomeric organization, contractile behaviour, electrical properties and response to ion channel-modulating compounds (as assessed by patch-clamp and optical voltage mapping). Moreover, differentiated iAMs had much narrower action potentials and propagated them at >10-fold higher speeds than the widely used murine atrial HL-1 cells. High-frequency electrical stimulation of confluent monolayers of differentiated iAMs resulted in reentrant conduction resembling atrial fibrillation, which could be terminated by tertiapin treatment, just like in monolayers of primary AMs.

Conclusion: Through controlled expansion and differentiation of AMs, large numbers of functional cardiomyocytes were generated with properties far superior to the differentiated progeny of existing cardiomyocyte lines. iAMs provide an attractive new model system for studying cardiomyocyte proliferation, differentiation, metabolism and (electro)physiology and to investigate cardiac diseases, regeneration and drug responses, without using animals.

Nonstandard abbreviations and acronyms

AMs	neonatal rat atrial cardiomyocytes
AF	atrial fibrillation
ANP	atrial natriuretic peptide
AP	action potential
APD	action potential duration
CV	conduction velocity
Cx43	connexin 43
dox	doxycycline
eGFP	enhanced green fluorescent protein
iAMs	conditionally immortalized AMs
IFM	immunofluorescence microscopy
LT	large T
LUMC	Leiden University Medical Center
LV	lentiviral vector
Mlc2a	atrial regulatory myosin light chain
Mlc2v	ventricular regulatory myosin light chain
pAMs	primary AMs
pVMs	primary neonatal rat ventricular cardiomyocytes
PSC-CMCs	cardiomyocytes derived from pluripotent stem cells
RMP	resting membrane potential
RT-qPCR	reverse transcription-quantitative polymerase chain reaction
SV40	simian virus 40

Introduction

Due to the limited availability of human heart tissue and the low mitotic activity of postnatal human cardiomyocytes, cardiac research has strongly relied on experiments in animals^{1,2} or with primary cardiomyocytes of animal origin^{3,4}. The increasing opposition to the use of animals for biomedical research has fuelled the search for alternative models of human cardiac disease.

Recently, cardiomyocytes derived from pluripotent stem cells (PSC-CMCs) have emerged as new models for studying different aspects of cardiac disease. Despite the great potential of PSC-CMCs as cardiac model systems, they have some serious drawbacks that need to be overcome before becoming a practical alternative to the use of laboratory animals. Both the generation of PSCs and the production of homogeneous populations of cardiomyocytes from these cells is a laborious, time-consuming and costly endeavour of varying efficiency, which requires properly timed treatment of the starting material with different cocktails of expensive growth factors and small molecules⁵. Moreover, PSCs greatly differ in their ability to differentiate into cardiomyocytes and typically yield phenotypically heterogeneous populations of immature cardiac muscle cells^{6,7}. The latter feature is limiting the use of PSC-CMCs in studying cardiac physiology and pathology, *e.g.* it has been proven difficult to establish homogeneous (confluent) monolayers of these cells for cardiac arrhythmia research by high-resolution optical mapping⁸.

As another approach to reduce laboratory animal use in cardiac research, cardiomyocyte lines have been generated using cardiac muscle cells from rodents and humans as starting material and the simian virus 40 (SV40) large T (LT) antigen to induce cell proliferation⁹⁻¹⁵. Unfortunately, all cardiomyocyte lines generated thus far, including the widely used HL-1 cell line, display large structural and functional deficits in comparison to the primary cells from which they were derived.

In an attempt to overcome the paucity of cell lines with robust cardiomyogenic differentiation capacity, we developed a new strategy to selectively and conditionally immortalize cardiomyocytes. Given our special interest in atrial fibrillation (AF) as the most common heart rhythm disorder in clinical practice¹⁶, the recent discovery by members of our research group that neonatal rat atrial cardiomyocytes (AMs) possess a constitutively active acetylcholine-dependent K^+ current playing an important role in the development of AF¹⁷ and the relatively low cell yields obtained from enzymatically dissociated neonatal rat atria, AMs were chosen as starting material. These cells were transduced with a single lentiviral vector (LV) allowing myocyte-restricted doxycycline (dox)/tetracycline-dependent LT expression followed by their clonal expansion in the presence of dox. The resulting monoclonal cell lines were characterized by cell proliferation assays, reverse transcription-quantitative polymerase chain reaction (RT-qPCR) analysis, phase-contrast and immunofluorescence microscopy (IFM), western blotting, optical voltage mapping. The response of the cells to cardiac ion channel inhibitors and their ability to integrate with pAMs were also investigated. Altogether, our data show that we have generated cardiomyocyte lines that (i) outperform all existing lines of cardiac muscle cells in terms of cardiomyogenic differentiation ability, (ii) have great potential as models for fundamental and applied cardiac research and (iii) depending on the specific

application, may provide easy-to-use and cost-effective alternatives for PSC-CMCs and for cardiomyocytes freshly isolated from animals.

Methods

Detailed methods are available in Supplementary material online.

Animal experiments

All animal experiments were approved by the Animal Experiments Committee of Leiden University Medical Center (LUMC) and conformed to the Guide for the Care and Use of Laboratory Animals as stated by the US National Institutes of Health.

Cardiac cell culture

Neonatal rat cardiomyocytes were isolated and cultured essentially as described¹⁸.

LV production

LV particles were produced using a previously published method¹⁸. The molecular structure of the shuttle plasmid used for the production of the LT-encoding LV is depicted in *Figure 1A*.

Molecular analyses

The primer pairs used for transcriptome analysis by RT-qPCR are shown in *Table S1* (see Supplementary material online).

Details about the antibodies used for western blotting and immunostaining of formaldehyde-fixed cells are presented in *Table S2* (see Supplementary material online).

Apoptosis was studied using Alexa Fluor-568-conjugated annexin V.

Electrophysiological studies

Optical voltage mapping using di-4-ANEPPS as fluorescent voltage indicator was performed essentially as described previously¹⁹. A detailed description of the whole-cell patch-clamp studies can be found in the Supplementary material online.

Statistical analyses

Data were derived from a specified number (N) of observations from 3 different cell cultures. Unless otherwise stated, data were expressed as mean±standard deviation (SD) and SDs were represented by error bars. All data were analysed with the nested ANOVA test using the Real Statistics Resource Pack software (release 5.1, copyright 2013 – 2017, Charles Zaiontz, www.real-statistics.com). For comparisons involving >2 experimental groups, this test was followed by Bonferroni *post-hoc* analysis. Results were considered statistically significant at *P* values <0.05. Statistical significance was expressed as follows: *: *P*<0.05, **: *P*<0.01, ***: *P*<0.001, ****: *P*<0.0001.

Results

Conditional immortalization of AMs

Low-density cardiomyocyte-enriched cultures of primary cells isolated from the atria of 2-day-old Wistar rats were transduced with LV particles containing a dox-inducible LT expression unit based on the monopartite lentiviral Tet-on system developed by Szulc *et al.*²⁰. LT expression in this LV system was driven by the strong hybrid striated muscle-specific MHCK7 promoter²¹ (*Figure 1A*) to minimize the likelihood of inadvertently immortalizing the $\pm 12\%$ non-cardiomyocytes present in the primary atrial cell cultures¹⁷ (data not shown).

In the presence of dox, cells started to divide forming clearly discernible colonies at 1-3 weeks post-transduction (*Figure 1B*). Nine of >80 cell clones were randomly selected for testing the dox dependency of their proliferation ability. Cells of all 9 clones were actively dividing in the presence of dox and stopped doing so in its absence. To investigate whether these clones contained excitable cells, confluent monolayers were established, maintained in dox-free culture medium for 9 days and examined by optical voltage mapping. Following 1-Hz electrical stimulation, 7 of the 9 clones produced excitatory waves spreading from the pacing electrode to the opposite site of the culture dishes. Of these 7 clones, clone #5 showed the shortest action potential (AP) duration (APD) and highest conduction velocity (CV) and was therefore picked for further investigation. Western blot analysis and IFM showed expression of LT in this clone to be tightly and effectively controlled by dox (*Figure 1C-E*).

Comparison of the light microscopic morphology of the conditionally immortalized AMs (iAMs) with those of primary AMs (pAMs) revealed that the surface area of proliferating iAMs did not significantly differ from that of pAMs at culture day 1 (*Figure 2A and E*). Also, in near-confluent monolayers, iAMs that were kept for 9 days in dox-free medium closely resembled pAMs at culture day 9 in both size and appearance (*Figure 2A*).

In the presence of dox, $72.2 \pm 8.1\%$ of iAMs stained positive for the proliferation marker Ki-67, which percentage dramatically decreased upon dox removal (*Figure 2B and F*). Consistently, in the presence of dox, iAMs proliferated with an average doubling time of 38 h, whereas under differentiation conditions (*i.e.* in the absence of dox), the cell number slightly decreased with time (*Figure 2G*). As expected, in primary atrial cell cultures, the percentage of α -actinin⁺ cells expressing Ki-67 was very low indicating that the large majority of proliferating Ki-67⁺ cells in these cultures are non-cardiomyocytes (*Figure 2C and F*). Probing iAM cultures with fluorescently labelled annexin V for the presence of surface-exposed phosphatidylserine as marker of apoptosis revealed low signals in proliferating cultures, which slightly increased under differentiation conditions (*Figure 2D and H*) but did not noticeably differ from those in 9-day-old pAM cultures (*Figure 2D and H*).

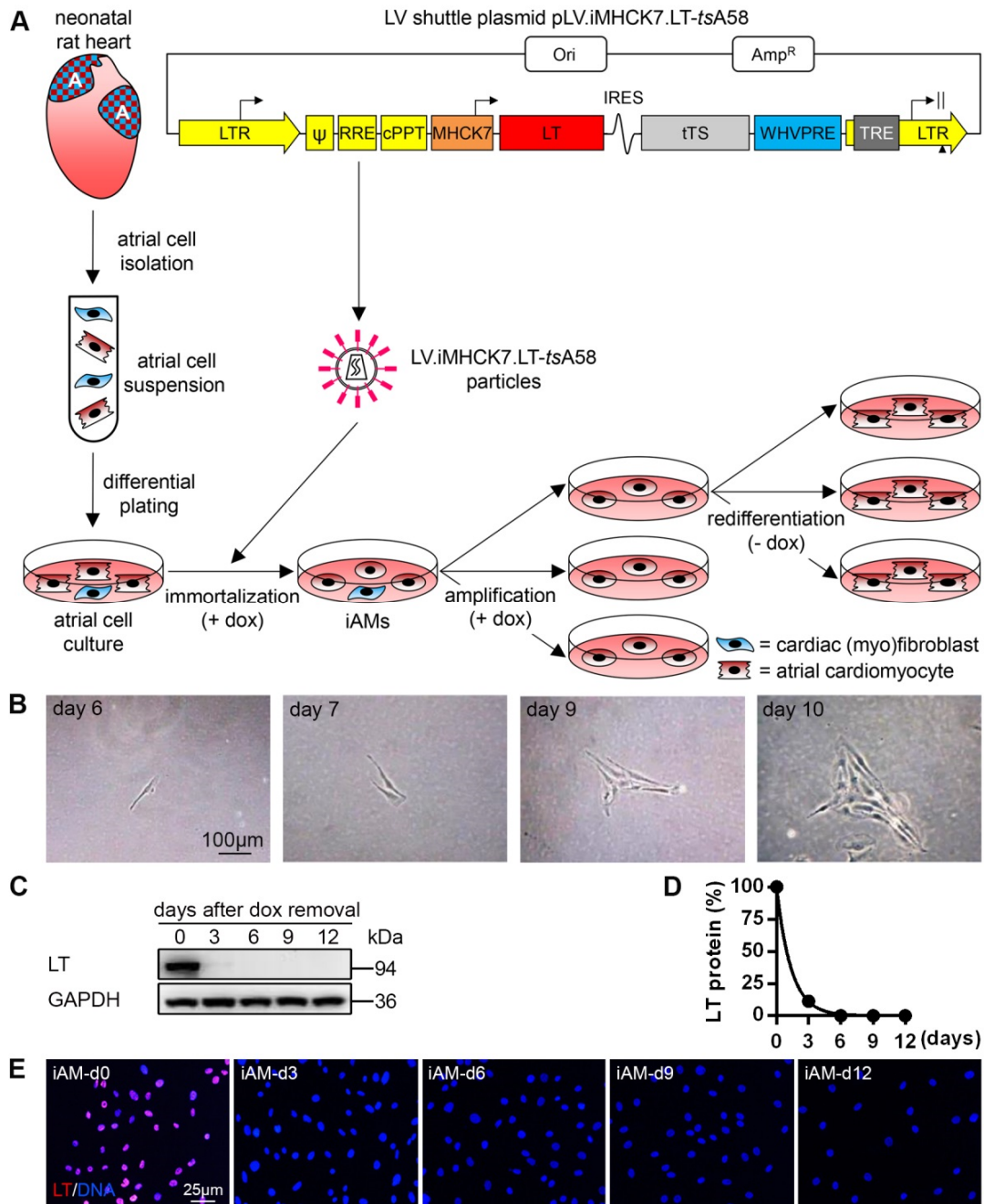


Figure 1. Conditional immortalization of pAMs. (A) Scheme of the procedure used for the reversible immortalization, amplification and subsequent redifferentiation of pAMs. A, atrium. Ori, bacterial origin of replication. Amp^R, *Escherichia coli* β -lactamase gene. LTR, human immunodeficiency virus type 1 (HIV1) long terminal repeat. Ψ , HIV1 packaging signal. RRE, HIV1 Rev-responsive element. cPPT, HIV1 central polypurine tract and termination site. MHCK7, chimeric striated muscle-specific promoter²¹. LT, coding sequence of the temperature-sensitive mutant LT protein tsA58³³. IRES, encephalomyocarditis virus internal ribosome entry site. tTS, coding sequence of the hybrid tetracycline-controlled transcriptional repressor TetR-KRAB³⁴. WHVPRE, woodchuck hepatitis virus posttranscriptional regulatory element. TRE, tetracycline-responsive promoter element consisting of 7 repeats of a 19 nucleotide tetracycline operator (*tetO*) sequence. (B) Bright-field images of a single cell in a pAM culture showing dox-dependent clonal expansion. (C-E) Analysis by western blotting (C, D) and immunocytochemistry (E) of LT protein expression in iAM cultures before (day 0) and 3, 6, 9 and 12 days after dox removal.

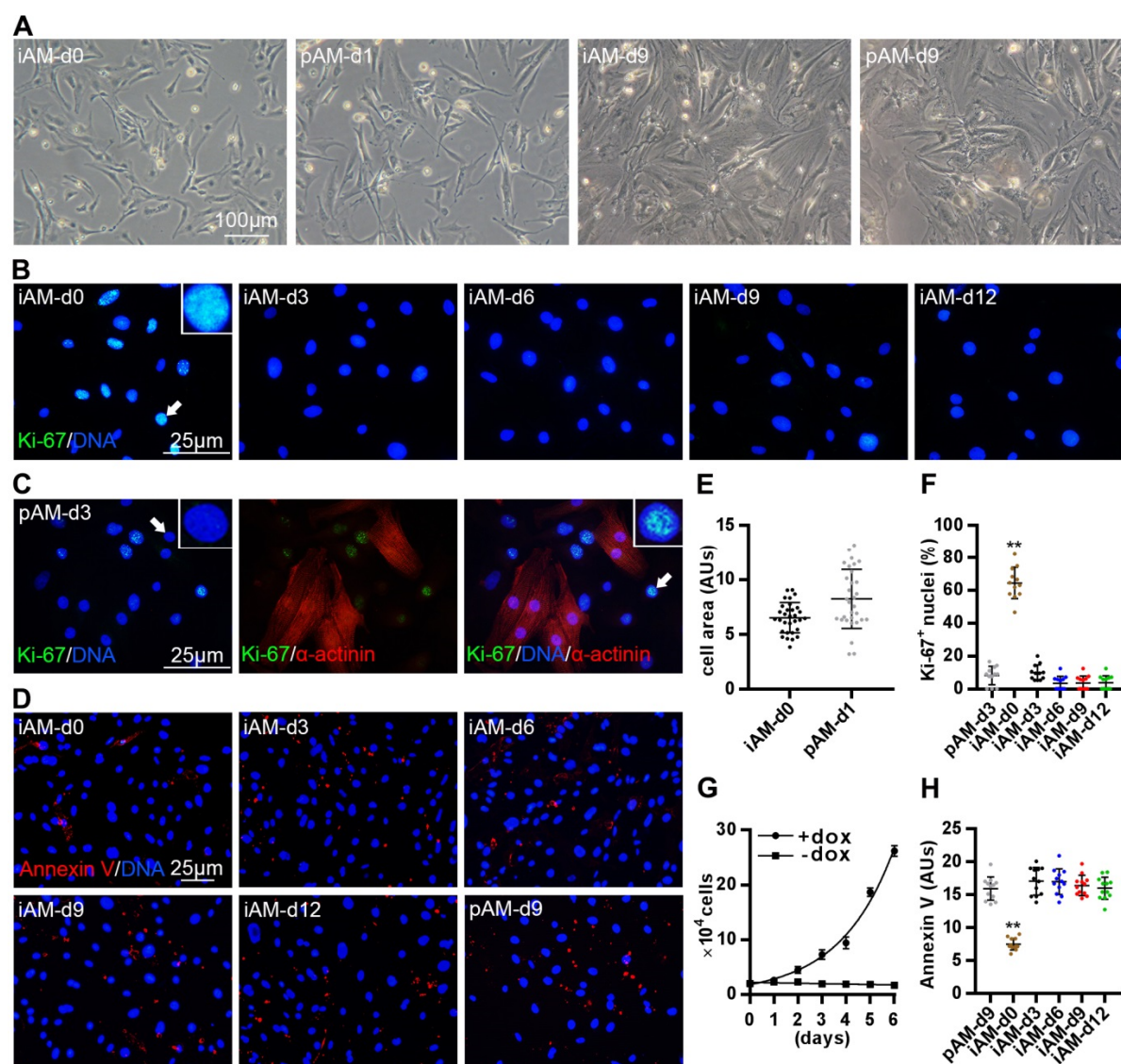


Figure 2. Morphology, proliferative activity and apoptosis analysis of iAMs. (A) Bright-field images of proliferating iAMs (*i.e.* iAM-d0) and iAM-d9 and of pAMs at culture day 1 (pAM-d1) and 9 (pAM-d9). (B) Fluorescence images of proliferating iAMs and of iAMs at different days after dox removal immunostained for the proliferation marker Ki-67. The arrow is pointing at the nucleus shown at a higher magnification in the inset. (C) Fluoromicrograph of a 3-day-old pAM (pAM-d3) culture that was not subjected to mitomycin C treatment following double immunostaining for Ki-67 and sarcomeric α -actinin. The Ki-67⁺/ α -actinin⁻ cells observed in this culture mainly result from uninhibited proliferation of cardiac fibroblasts (data not shown). Arrows are pointing at the nuclei shown at a higher magnification in the insets. (D) Fluorescence images of proliferating iAMs, of iAMs at different days after dox removal and of a 9-day-old, mitomycin C-treated pAM (pAM-d9) culture labelled with Alexa Fluor-568-conjugated annexin V to assess externalization of phosphatidylserine as indicator of apoptosis. (E) Quantification of cell surface area of iAM-d0 and of pAM-d1. Data are presented as mean \pm SD, N=30 cells per experimental group, each consisting of 3 cell preparations. For statistical analysis, the nested ANOVA test was used. (F) Graph showing the percentage of Ki-67⁺ nuclei in proliferating iAM cultures, in iAM cultures at different days after dox removal and among the cardiomyocytes (*i.e.* α -actinin⁺ cells) in pAM-d3 cultures. Data are presented as mean \pm SD, N=12 cell cultures per experimental group from 3 individual preparations. Statistics was done

using the nested ANOVA test with Bonferroni *post-hoc* correction. (G) Quantification of cell numbers in iAM cultures with or without dox. Data are presented as mean \pm SD, N=3. (H) Quantification of cell surface-bound annexin V in proliferating iAM cultures, in iAM cultures at different days after dox removal and in mitomycin C-treated pAM-d9 cultures. Data are presented as mean \pm SD, N=12 cell cultures per experimental group from 3 individual preparations. Statistics was done using the nested ANOVA test with Bonferroni *post-hoc* correction. AUs, arbitrary units. ** $P < 0.01$ vs pAM cultures.

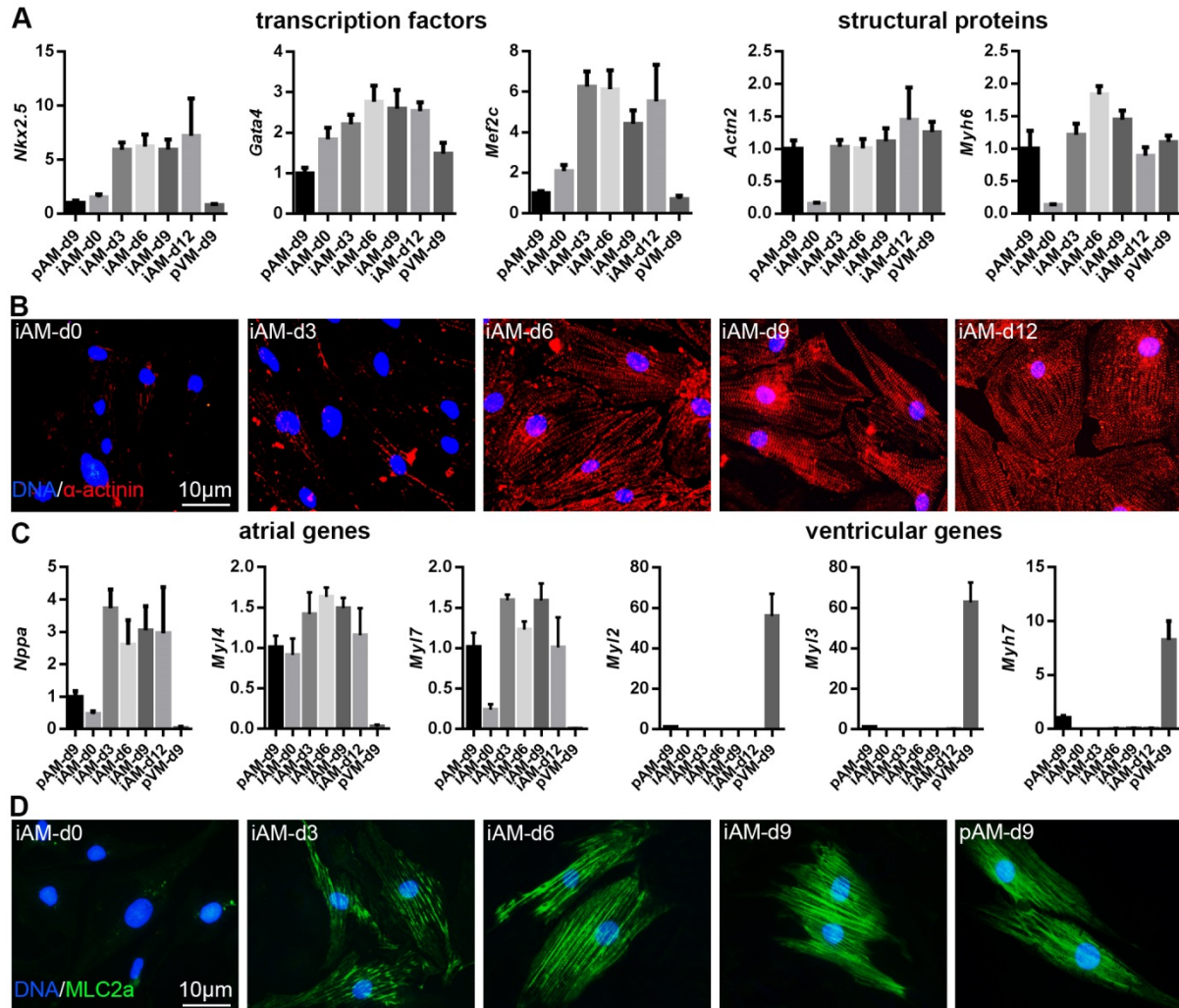


Figure 3. Cardiomyogenic differentiation potential of iAMs. (A, C) Analysis by RT-qPCR of the expression of the cardiac transcription factor genes *Nkx2.5*, *Gata4* and *Mef2c*, the cardiac sarcomeric protein genes *Actn2* and *Myh6* (A), the “atrial” genes *Nppa*, *Myl4* and *Myl7* and the “ventricular” genes *Myl2*, *Myl3* and *Myh7* (C) in pAMs and pVMs at day 9 of culture and in iAMs on the indicated days of differentiation. mRNA levels are expressed relative to those in 9-day-old pAM (pAM-d9) cultures, which were set at 1. Data are presented as mean \pm SD, N=3. The low abundance of “atrial” transcripts in pAM samples is most likely due to the presence of some ventricular myocytes in these samples. Similarly, the pVM cultures may have contained low numbers of atrial myocytes. Alternatively, pAMs may express “ventricular” genes at low levels and pVMs may display low-level expression of “atrial” genes. (B, D) Fluorescence images of proliferating iAMs and of iAMs at different days after dox removal immunostained for sarcomeric α -actinin (red, B) or the atrial regulatory myosin light chain MLC2a (green, D). pAMs and pVMs at culture day 9 served as positive and negative control for the MLC2a immunostaining, respectively. Cell nuclei have been visualized by staining with Hoechst 33342 (blue).

Cardiomyogenic differentiation potential of iAMs

The expression of cardiac marker genes in proliferating and differentiating iAM cultures was assessed by RT-qPCR analysis and compared with that of pAMs and of primary neonatal rat ventricular cardiomyocytes (pVMs) at culture day 9. Previous experience has shown that at this particular time point, the primary cardiomyocytes are optimally adapted to the *in vitro* environment and still in an advanced state of differentiation^{17-19,22,23}. Expression of the *Nkx2.5*, *Gata4* and *Mef2c* genes, which encode early cardiac transcriptional regulators, was higher in proliferating (*i.e.* day 0) iAMs than in pAMs and pVMs and rapidly increased soon after dox removal (*Figure 2A*). Expression of the sarcomeric protein-encoding *Actn2* and *Myh6* genes, on the other hand, was lower in day 0 iAMs than in pAMs and s. Transcription of these genes also showed a rapid increase under differentiation conditions to very similar levels as in pAMs and pVMs (*Figure 3A*).

To study myofibrillogenesis, cells were immunostained for sarcomeric α -actinin (*Figure 3B*). At the immortalized stage, α -actinin expression in iAMs was low and in most cells the protein was diffusely spread throughout the cytoplasm. However, in a few cells, α -actinin showed a punctate staining pattern with the protein clustering in spherical or short elongated structures. At day 3 of differentiation, α -actinin formed longer structures with a dot-like appearance reminiscent of immature myofibrils. Myofibril assembly nearly reached completion at day 6 after dox removal, with most of the α -actinin displaying the Z-line staining pattern typical of cardiomyocytes. At the later stages of differentiation (*i.e.* at days 9 and 12 after dox removal), myofibrils underwent further maturation resulting in cells with highly organized sarcomeres.

After dox removal, mRNA levels of the atrial natriuretic peptide (ANP)-encoding *Nppa* gene, the atrial essential myosin light chain-encoding *Myl4* gene and the atrial regulatory myosin light chain (*i.e.* Mlc2a)-encoding *Myl7* gene were moderately (*Myl4*) to strongly (*Nppa* and *Myl7*) upregulated in iAMs (*Figure 3C*). Moreover, neither in the absence nor in the presence of dox, iAMs expressed detectable amounts of transcripts encoding ventricular regulatory myosin light chain (*i.e.* Mlc2v; *Myl2* gene), ventricular essential myosin light chain (*Myl3* gene) or β -myosin heavy chain (*Myh7* gene; *Figure 3C*). The RNA samples of 9-day-old pAM cultures contained high amounts of "atrial" mRNA while "ventricular" transcripts were barely detectable in these samples (*Figure 3C*). For the RNA samples from the 9-day-old pVM cultures the opposite was true, *i.e.* they contained high amounts of *Myl2*, *Myl3* and *Myh7* transcripts but hardly any *Nppa*, *Myl4* or *Myl7* mRNA (*Figure 3C*). Collectively, these data indicate that iAMs reacquire properties of atrial rather than ventricular cardiomyocytes when cultured in dox-free medium (*Figure 3C*). Mlc2a immunostaining confirmed these findings and showed gradual incorporation of this protein into sarcomeres indiscernible from those in pAMs that had been cultured for 9 days (*Figure 3D*). iAMs started to exhibit spontaneous contractions from day 6 of differentiation (Supplementary material online, *Movie 1*) demonstrating sarcomere functionality. The immunostainings for α -actinin and Mlc2a also revealed that the spontaneous differentiation of iAMs in the absence of dox is a highly synchronous event occurring in essentially all cells at approximately the same time.

Electrophysiological properties of iAMs

RT-qPCRs targeting genes encoding cardiac ion channels showed an increase in the mRNA levels of *Scn5a*/*Nav*_v1.5, *Cacna1c*/*Ca*_v1.2, *Kcnj3*/*K*_{ir}3.1, *Kcnj5*/*K*_{ir}3.4 and *Kcnj11*/*K*_{ir}6.2 during the early stages of iAM differentiation, which, later in the differentiation process, dropped to approximately equal levels as in pAMs at culture day 9 (Supplementary material online, *Figure S1A-E*). A similar differentiation-dependent trend in expression levels was observed for *Kcnd3*/*K*_v4.3 and *Kcnh2*/*K*_v11.1 but in these cases transcript levels at the late stages of iAM differentiation were higher than those in day 9 pAMs (Supplementary material online, *Figure S1F and G*). The iAMs did not express detectable amounts of *Kcnj2*/*K*_{ir}2.1 at any stage in the differentiation process in contrast to pAMs that had been cultured for 9 days (Supplementary material online, *Figure S1H*). However, *Kcnj2* expression in pAMs was much lower than in pVMs at culture day 9. Transcript levels of the pacemaker channel genes *Hcn2* and *Hcn4* showed dynamic changes during the cardiomyogenic differentiation of iAMs (Supplementary material online, *Figure S1I and J*). Proliferating iAMs expressed more *Hcn2* mRNA than pAMs at day 9 of culture but this difference largely disappeared following 12 days of cardiomyogenic differentiation of the iAMs. The *Hcn4* mRNA level in proliferating iAMs was lower than in pAMs at culture day 9 but showed a gradual increase during the first 9 days of iAM differentiation to suddenly drop afterwards. RT-qPCR analysis of *Ryr2* and *Atp2a2*/*Serca2* transcripts showed an increase in the expression of these Ca²⁺-handling protein genes early during iAM differentiation. From day 3 of differentiation onwards, *Ryr2* and *Atp2a2* mRNA levels in iAMs remained constant and were very similar (*Ryr2*) or 2- to 3-fold higher (*Atp2a2*) than in pAMs at culture day 9 (Supplementary material online, *Figure S1K and L*).

Since spreading of APs through cardiac tissue critically depends on the presence of intercellular conduits, iAM cultures at different stages of differentiation were immunostained for the gap junction protein connexin 43 (Cx43). As shown in *Figure 4A*, Cx43 was first observed in iAMs at 3 days after dox removal and its amounts gradually increased as the cells further differentiated. Initially, Cx43 was mainly detected in the perinuclear region (*i.e.* at the site of biosynthesis) but at days 9 of differentiation, most Cx43 was found in punctate patterns at the interfaces between iAMs. To investigate the functionality of these gap junctional plaques, confluent monolayers of differentiated iAMs were subjected to 1-Hz electrical point stimulation, which caused the cells to contract at the pacing frequency (Supplementary material online, *Movie II*). This result was corroborated by optical voltage mapping, which showed uniform radial spreading of excitatory waves from the site of electrical point stimulation in iAM cultures at day 9 of differentiation (Supplementary material online, *Movie III*). Additional optical voltage mapping experiments revealed a gradual increase in CV (*Figure 4B and D*; Supplementary material online, *Movie III*) and decrease in APD (*Figure 4C, E and F*) with ongoing iAM differentiation. As a matter of fact, CV and APD at 30 and 80% repolarization (APD₃₀ and APD₈₀, respectively) did not significantly differ between iAM cultures at differentiation days 9 and 12 and 9-day-old pAM cultures. These data suggest that upon dox removal, iAMs differentiate into AMs with electrophysiological properties strongly resembling those of pAMs.

To investigate the ionic basis of the similar electrophysiological properties of pAMs and cardiomyogenically differentiated iAMs as measured by optical voltage, we conducted patch-clamp experiments on these cardiomyocytes. The resting membrane potentials (RMP) of pAMs and iAMs in monolayer culture did not significantly differ (-64.5 ± 1.2 mV, $N=15$ vs -67.5 ± 1.6 mV, $N=13$), while single-cell recordings showed pAMs to have a more negative RMP (-62.8 ± 1.8 mV, $N=14$) than iAMs (-46.0 ± 1.9 mV, $N=27$; Supplementary material online, Figure S2A). In spite of the measured difference in RMP between single pAMs and single iAMs, both cell types were excitable and produced APs with very similar characteristics under the same stimulation conditions (Supplementary material online, Figure S2B and Table S3). Of all the AP parameters assessed only the upstroke velocity and the overshoot were somewhat smaller for the iAMs in comparison to the pAMs (Supplementary material online, Table S3). In voltage-clamp experiments, we found that the main membrane current responsible for the excitability of both cell types is a fast voltage-activated transient Na^+ current (consistent with the expression of *Scn5a* in these cells, Supplementary material online, Figure S1A), which occurred in these cells as a dominant current component (see Supplementary material online, Figure S2B, D and E). Although these patch-clamp results fit with the optical mapping data, we were puzzled by the similar RMPs for pAM and iAM monolayers, given the undetectable *Kcnj2* expression in cardiomyogenically differentiated iAMs (Supplementary material online, Figure S1H) and the presumed difference in the inward rectifier current between pAMs and iAMs (I_{K1} ; Supplementary material online, Figure S2B). This apparent discrepancy was resolved by showing, with the aid of ouabain, that the electrogenic Na^+/K^+ ATPase plays a vital role in generating hyperpolarized RMPs in both pAMs and iAMs (Supplementary material online, Figure S3).

To investigate their ability to form a functional cardiac syncytium with pAMs, iAMs were labelled with enhanced green fluorescent protein (eGFP) by lentiviral transduction. Next, 1:1 co-cultures of pAMs treated at day 1 of culture with mitomycin C and eGFP-labelled iAMs were established and subsequently kept for 8 days in dox-free culture medium. The co-cultures were compared with iAM monocultures at day 9 of differentiation and with 9-day-old, mitomycin C-treated pAM cultures. (Supplementary material online, Figure S4A). Cx43 immunostaining of the co-cultures revealed the presence of gap junctions between iAMs and pAMs (Supplementary material online, Figure S4B). Optical voltage mapping showed uniform radial spreading of APs from the pacing electrode at roughly the same speed in all 3 culture types (Supplementary material online, Figure S4C and D) suggesting proper electrical integration of differentiated iAMs in co-cultures with pAMs.

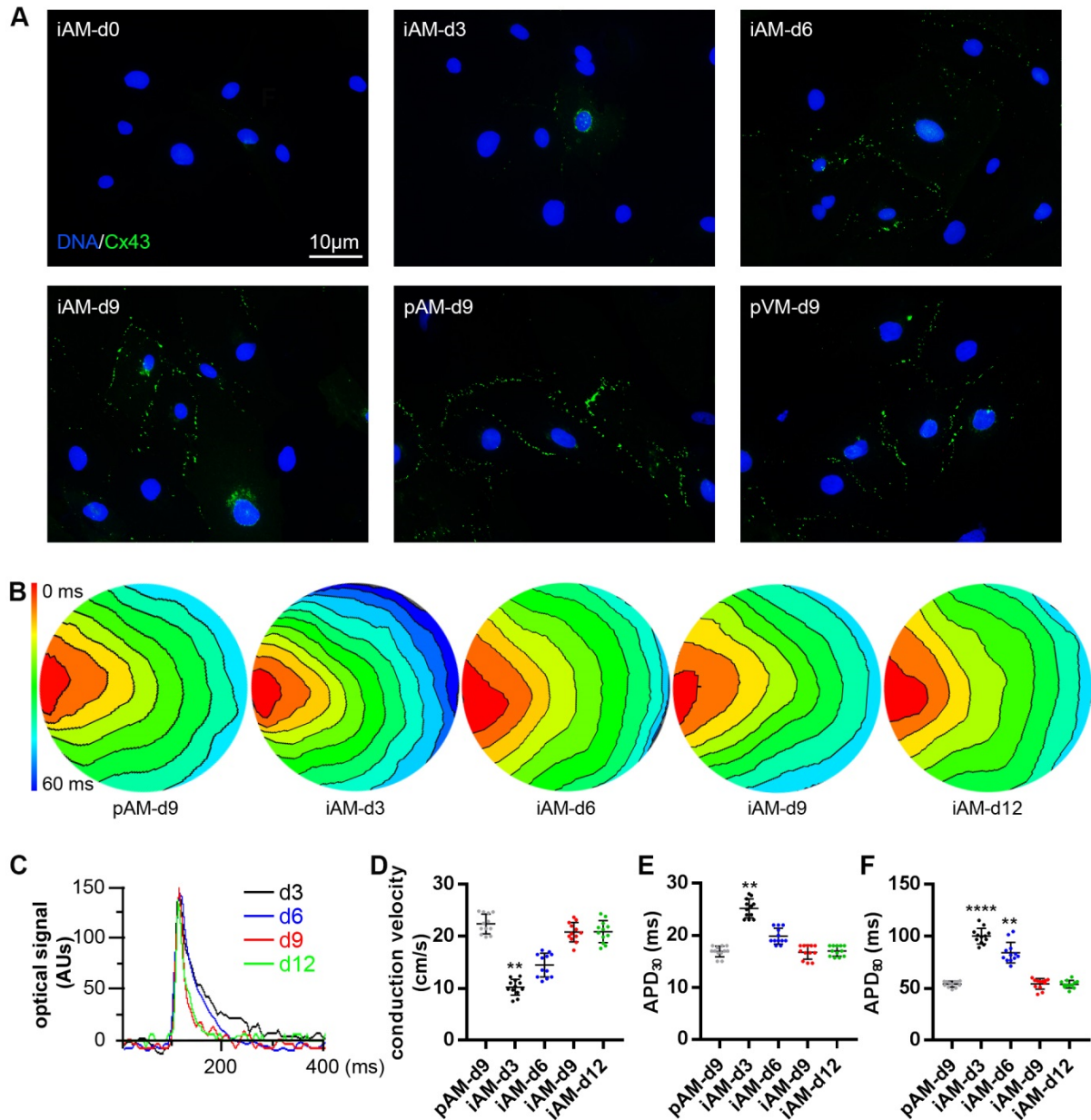


Figure 4. Electrophysiological properties of iAMs. (A) Fluorescence images of proliferating iAMs and of iAMs at different days after dox removal immunostained for Cx43 (green) showing its differentiation-dependent accumulation at the sarcolemma in gap junctional plaques. As positive controls for the Cx43 immunostaining, 9-day-old pAM and pVM cultures were included. Hoechst 33342 (blue) staining shows cell nuclei. (B-F) Optical voltage mapping of confluent iAM and 9-day-old pAM (pAM-d9) monolayers following 1-Hz electrical point stimulation. (B, C) Typical activation maps (B; isochrones are separated by 6 ms) and optical signal traces (C) of iAM cultures at different days after dox removal showing an increase in CV and a decrease in APD with advancing iAM differentiation. (D-F) Quantification of CV (D), APD₃₀ (E) and APD₈₀ (F) in pAM-d9 cultures and in iAM cultures at 3, 6, 9 and 12 days of differentiation. Data are presented as mean±SD, N=12 cell cultures per experimental group from 3 individual preparations. Statistics was done using the nested ANOVA test with Bonferroni *post-hoc* correction. AUs, arbitrary units. ** $P < 0.01$ and **** $P < 0.0001$ vs pAM-d9 cultures.

Comparison of the electrophysiological properties of iAMs and HL-1 cells

The electrophysiological properties of iAM clone #5 were compared with those of the widely used HL-1 cell line, which was derived from the AT-1 mouse atrial myocyte tumour lineage¹¹. To this end, confluent monolayers of iAMs at day 9 of differentiation and optimally maintained confluent cultures of HL-1 cells were subjected to optical voltage mapping following 1-Hz pacing. The CV in the HL-1 cultures was ± 20 -fold lower than in the iAM cultures (*Figure 5A* and *B*; *Movie III*) and HL-1 cells displayed greatly prolonged APs as compared to differentiated iAMs (*Figure 5C*) characterized by a very slow upstroke. These data clearly demonstrate that differentiated iAMs possess electrophysiological properties superior to those of HL-1 cells.

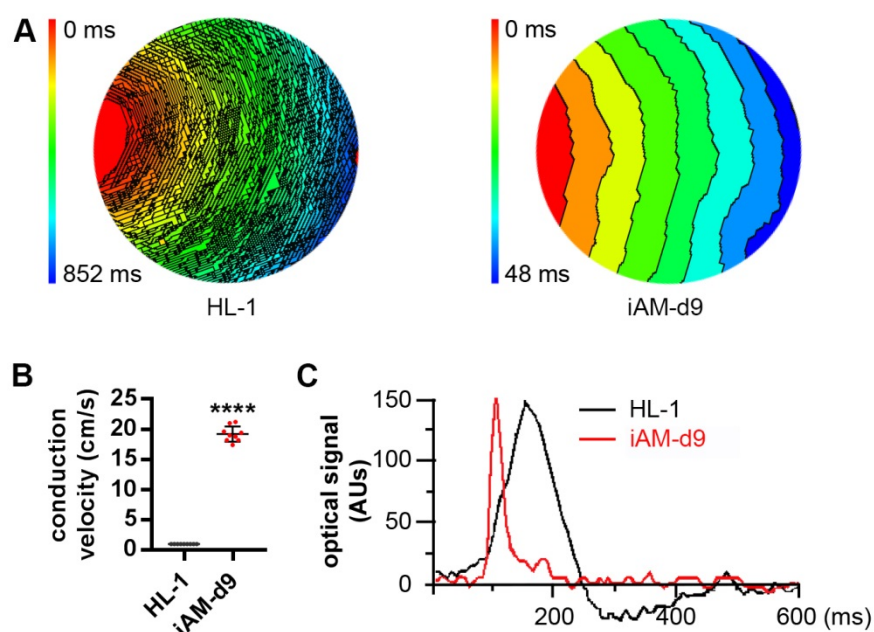


Figure 6. Comparison by optical voltage mapping and 1-Hz electrical point stimulation of the electrophysiological properties of confluent monolayers of iAMs at day 9 of differentiation (iAM-d9) with those of HL-1 cells. Typical activation maps (*A*, 6-ms isochrone spacing) showing a much slower CV (*B*) and optical signal traces (*C*) showing a much longer APD for the HL-1 cells as compared to the iAM-d9. Data are presented as mean \pm SD, N=9 cell cultures per group from 3 individual preparations. For statistical analysis, the nested ANOVA test was used. AUs, arbitrary units. **** P <0.001.

iAMs as *in vitro* model of AF

Our research group previously developed an *in vitro* model of AF based on high-frequency electrical stimulation of confluent pAM cultures. The resulting reentrant circuits, or so-called rotors, could be terminated by prolonging APD of the pAMs using the $K_{ir}3.x$ -specific inhibitor tertiapin¹⁷. To determine whether confluent cultures of iAMs at different stages of differentiation would display similar behaviour, they were burst paced in the absence or presence of 100 nM tertiapin. While rotors could be readily induced in iAM cultures from differentiation day 6 onwards (*Figure 6A-C*; Supplementary material online, *Movie IV*), reentry could not be established in iAM cultures at day 3 of differentiation (*Figure 6C*). Reentry inducibility, the number of rotors per culture and rotor frequency increased with the time after dox removal

(Figure 6C-E). After treatment with tertiapin, iAMs that had been cultured for 9 days without dox showed a strong increase in APD (Figure 6F-H). Moreover, in the presence of tertiapin it was no longer possible to induce reentry in confluent monolayers of iAMs at day 6, 9 or 12 of differentiation by burst pacing (Figure 6C-F). The fact that tertiapin treatment only slightly reduced the CV in confluent monolayers of iAMs at day 9 of differentiation (from 20.5 to 19.8 cm/s; Figure 6I) suggests that Kir3.x channel activity is not the major determinant of iAM excitability at the monolayer level.

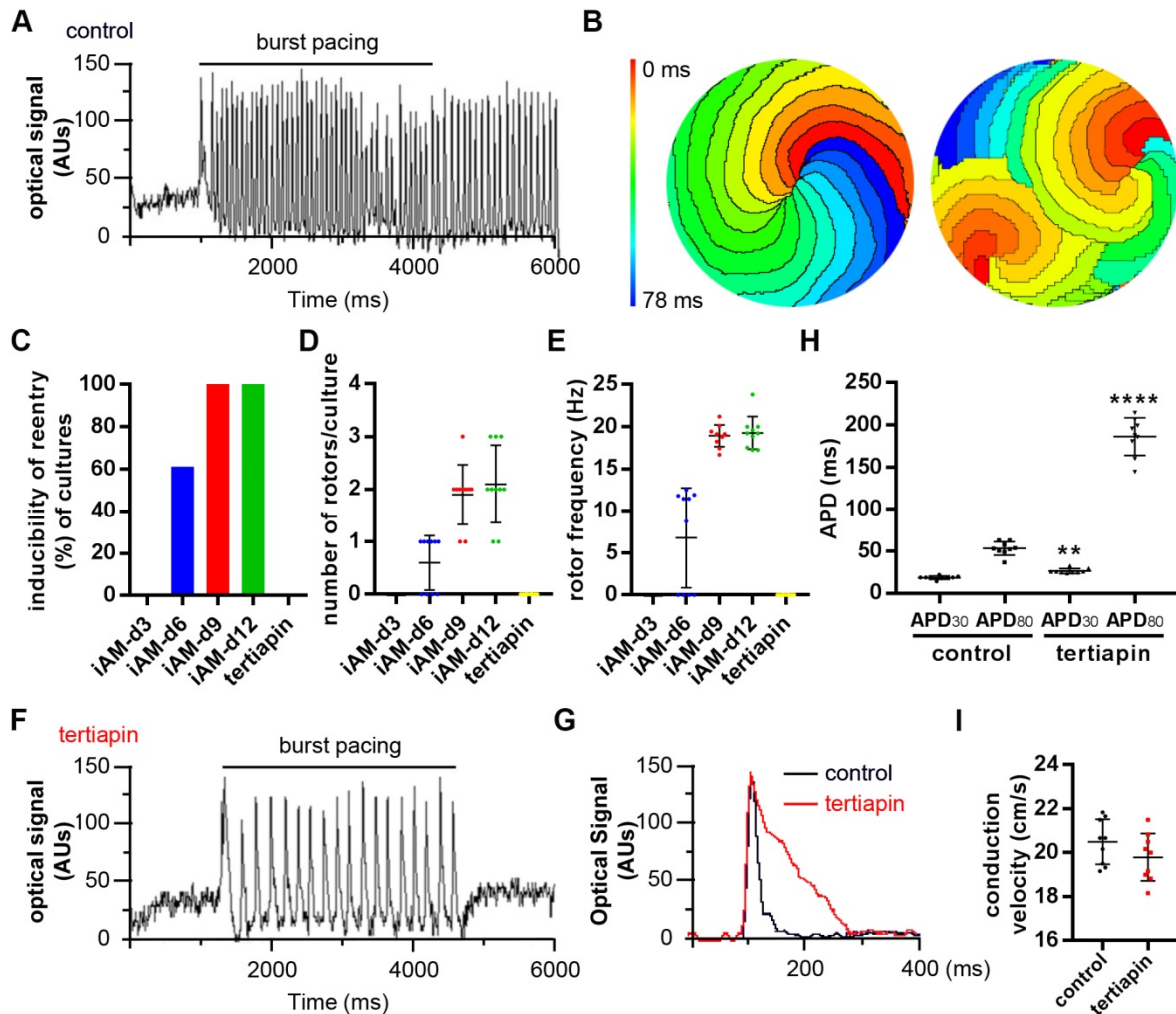


Figure 5. Suitability of iAMs as *in vitro* AF model assessed by optical voltage mapping.

(A, F) Typical optical signal traces of mock- (A) and tertiapin (F)-treated iAMs at day 9 of differentiation (iAM-d9) after high-frequency (10-50 Hz) electrical point stimulation. (B) Activation maps (6-ms isochrone spacing) of iAM-d9 cultures showing 1 (left) or 2 (right) reentrant circuits. (C-E) Inducibility of reentry (C), arrhythmia complexity (D) and quantification of rotor frequency (E) in iAM cultures at 3, 6, 9 and 12 days of differentiation. (G) Typical optical AP records of mock- (black) and tertiapin (red)-treated iAM-d9 following 1-Hz pacing. (H-I) Quantification of APD₃₀, APD₈₀ (H) and CV (I) of mock- and tertiapin-treated iAM-d9. Data are presented as mean±SD, N=9 cell cultures per experimental group from 3 individual preparations. Statistics was done using the nested ANOVA test with Bonferroni *post-hoc* correction. ** $P < 0.01$ and **** $P < 0.0001$ vs control cultures.

Discussion

Until now, all attempts to generate lines of cardiomyocytes that can give rise to cells with electrical and contractile properties approaching those of the starting material have failed. Indeed, all cardiomyocyte lines reported to date display large structural and functional deficits compared to the primary cardiomyocytes from which they were derived^{11,13,15,24}. In this study, we have solved this problem and describe the generation of monoclonal lines of conditionally immortalized neonatal rat atrial myocytes with preserved cardiomyogenic differentiation capacity. This was accomplished by transducing pAMs with an LV directing myocyte-selective and dox-dependent expression of the SV40 LT antigen. Culturing of the resulting cells in medium with dox caused their rapid expansion, while in dox-free culture medium, the amplified cells spontaneously and synchronously differentiated into fully functional (*i.e.* excitable and contractile) AMs that were successfully used to develop a monolayer model of AF, for investigating the APD-prolonging effects of toxins (tertiapin, *Figure 6*). To provide our iAMs with a unique and easy-to-remember identifier, we have dubbed the progeny of iAM clone #5 the iAM-1 cell line.

Properties of iAMs

RT-qPCR analysis of iAMs in different stages of differentiation (*Figure 3* and Supplementary material online, *Figure S1*) shows a rapid increase in mRNA levels of cardiac transcription factors, ion channels, Ca²⁺-handling proteins and sarcomeric proteins shortly after dox removal. At later stages of differentiation, these mRNA levels generally either stay fairly constant (as for the genes encoding cardiac transcription factors, sarcomeric and Ca²⁺-handling proteins and ANP) or decline again to the approximate mRNA levels of pAMs (*Scn5a*, *Cacna1c*, *Hcn2*, *Kcnj3*, *Kcnj11*) and/or proliferating iAMs (*Scn5a*, *Cacna1c*, *Kcnd3*, *Kcnh2*, *Kcnj3*). These findings are consistent with the notion that upon dox removal iAMs rapidly engage in a cardiomyogenic differentiation program with the concomitant upregulation of genes needed to build a functional cardiomyocyte. To complement the RT-qPCR data, we recently initiated an RNA-seq study focussing on transcriptomes of iAMs at different stages of cardiomyogenic differentiation and subsequent dedifferentiation. The results of this study will be presented elsewhere.

Following their differentiation in the absence of dox, iAMs acquire properties of atrial rather than ventricular myocytes as evinced by the high-level expression in differentiated iAMs of “atrial” genes including *Nppa*, *Myl4*, *Myl7*, *Kcnj3* and *Kcnj5*¹⁷ and the lack of expression of the “ventricular” *Myl2*, *Myl3* and *Myh7* genes²⁵. Moreover, following 1-Hz pacing, differentiated iAMs display rapid contractions that strongly resemble those of pAMs but are quite different from the slower contractions of pVMs (Supplementary material online, *Movie II* and data not shown). Consistently, the average APD₃₀ and APD₈₀ of differentiated iAMs do not significantly differ from those of pAMs (*Figure 4E* and *F*, respectively; Supplementary material online, *Table S3*) but are much shorter than the average APD₃₀ and APD₈₀ of pVMs (Supplementary material online, *Figure S5*). Collectively, these findings indicate that although LT expression results in the dedifferentiation and proliferation of AMs, the cells retain

some kind of epigenetic memory causing them to spontaneously differentiate into atrial myocytes upon dox removal.

RMPs of iAMs and pAMs

pAM and iAM monolayers had similar RMPs (*Figure S2A*). Although RMP measurements of single cells are less reliable than those of cell clusters, because the voltage is measured from a high-resistance source ($R_m > 100 \text{ M}\Omega$) after establishing giga-seal, the RMPs of single pAMs and pAM monolayers did not significantly differ (*Figure S2A*). However, the RMP of single iAMs was significantly depolarized compared to that of iAM monolayers (*Figure S2A*). Further experiments as part of a dedicated patch-clamp study are needed to determine the precise cause for this difference, which may, however, relate to the lack of *Kcnj2* expression in cardiomyogenically differentiated iAMs (*Figure S1H*) together with technical difficulties to perform meaningful RMP measurements in neonatal/immature (atrial) cardiomyocytes due to their high plasma membrane resistance^{26,27}.

Our finding that the electrogenic Na^+/K^+ ATPase plays an important role in the generation of the RMP of AMs is of particular interest, because it ensures a sufficiently negative RMP for the maintenance of excitability of iAMs in monolayer cultures, in the absence of *Kcnj2* expression. The great importance of the Na^+/K^+ pump for establishing physiological Na^+ and K^+ gradients is widely recognized in the electrophysiology of adult cardiomyocytes. Decreased activity of the Na^+/K^+ pump under ischaemic conditions causes the loss of physiological K^+ and Na^+ gradients with consequent RMP depolarization and other effects favouring arrhythmogenesis²⁸. However, as stated in many physiology textbooks, a direct contribution of the electrogenic action of the Na^+/K^+ pump to the RMP of adult cardiomyocytes is often considered as relatively small compared to the pump's indirect electrogenic effect, *i.e.* its ability to create transmembrane K^+ and Na^+ gradients. This may be understood by considering the Na^+/K^+ pumps in the plasma membrane as a low conductance pathway with a negative reversal potential determined by their ATP-driven action^{29,30}. This implies that the direct electrogenic effects of pump currents will, at the same current densities, be more prominent in high-resistance ($\sim 1 \text{ G}\Omega$) cardiomyocytes like the AMs than in lower-resistance ($\sim 100 \text{ M}\Omega$) cardiomyocytes like adult rat ventricular cardiomyocytes³¹. Possibly, no/low expression of inward rectifier K^+ channels in iAMs and an important role for the Na^+/K^+ ATPase activity in setting the RMP is characteristic for young (atrial) myocytes or a sign of incomplete differentiation of these cells. Developmental increases in I_{K1} are not uncommon and have previously been reported for ventricular cardiomyocytes of various rodent species³².

Because of the dominance of voltage-activated Na^+ channels in the voltage-clamp recordings of both pAMs and iAMs, we ascribed the excitability of iAMs mainly to those channels. However, AMs also express, though at much lower levels, voltage-activated Ca^{2+} channels³³ (Supplementary material online, *Figure S1B*), which may be expected to contribute to pAM and iAM excitability. How these Ca^{2+} channels compare in their contribution to excitability in pAMs and iAMs deserves further experimental work. The same applies to the contributions of outward rectifier K^+ currents to the excitability of pAMs and iAMs, and to the realisation of the RMP of single iAMs in general.

Possible applications of iAMs

Long-term culture of iAMs did not significantly reduce their proliferation rate in the presence of dox and the sarcomeric organization and contractile behaviour of iAMs from different passages at day 9 of differentiation were indistinguishable (data not shown). Moreover, no progressive cell flattening, nuclear enlargement, development of senescence-associated heterochromatin foci or other signs of senescence were observed during the first 55 population doublings of the cells. Assessment of the electrophysiological properties of confluent monolayers of differentiated iAMs by optical voltage mapping after 25, 40 and 55 population doublings revealed no significant differences in APD or CV (see Supplementary material online, *Figure S6*). Also, differentiated iAMs resume cell division following addition of dox to the culture medium and redifferentiate again into atrial myocytes following subsequent dox removal (data not shown). iAMs therefore provide a virtually unlimited supply of cardiomyocytes for fundamental research but may also prove very useful for: (i) the development of acquired disease models, (ii) identifying new therapeutic targets, (iii) screening of drugs and toxins, (iv) testing of new treatment modalities (*e.g.* gene and cell therapy), (v) production of biopharmaceuticals in bioreactors or encapsulated cell/tissue grafts and (vi) the improvement of tissue engineering approaches. The recent rapid progress in genome editing technologies³⁴ will further expand the applicability of iAMs allowing them to be used as models for studying key aspects of inherited cardiomyopathies.

A highly attractive feature of the iAMs is that they spontaneously undergo cardiomyogenic differentiation in a synchronous and near quantitative manner in standard culture medium without dox. Contrarily, generation of cardiomyocytes from embryonic or induced PSCs requires their properly timed treatment with various cocktails of growth factors and small molecules⁵. This typically yields phenotypically heterogeneous populations of mostly immature cardiomyocytes contaminated with variable percentages of non-cardiomyocytes. Consequently, to obtain relatively pure populations of PSC-CMCs various different enrichment procedures have been developed³⁵. Production of more or less homogeneous populations of cardiomyocytes from PSCs thus is a laborious, time-consuming and costly endeavour as compared to the straightforward generation of atrial myocytes from iAMs. This may explain why there are very few reports on the use of PSC-CMCs to investigate cardiac arrhythmias in monolayer cultures by optical mapping⁸, while such experiments are easily performed with differentiated iAM monolayers (*Figure 4-6* and Supplementary material online, *Figure S3-9*). Also, in contrast to PSC-CMCs, iAMs offer the possibility to study the molecular mechanisms involved in the transition of a differentiated cardiomyocyte that is no longer able to undergo cytokinesis into an actively dividing cell. This is particularly relevant given the growing interest in the regeneration of mammalian hearts from within by stimulating cardiomyocytes surrounding the site(s) of cardiac injury to multiply themselves through cell division^{36,37}. Current findings regarding the molecular changes accompanying the reactivation of cardiomyocyte proliferation should be interpreted with caution due to the presence of other cell types (*e.g.* cardiac fibroblasts and inflammatory cells) in most test materials. iAMs do not suffer from this drawback making them a potentially

highly useful model system to study the mechanisms underlying cell cycle reentry and progression of cardiomyocytes.

Optical voltage mapping of other clones of excitable iAMs yielded very similar results although not all of them reached the same maximum CV and minimum APD as clone #5 (e.g. clone #1 and #6; Supplementary material online, *Figure S7A-C* and *D-F*, respectively). An intriguing finding of this study is the difference in electrophysiological properties between the differentiated progeny of different iAM clones, which extends to iAM clones not presented in this study. The cause(s) of this heterogeneity is/are unclear given the fact that cardiomyogenically differentiated cells with a similarly high level of sarcomeric organization still differed in electrophysiological behaviour (data not shown). Therefore, besides a different propensity to mature, other factors might explain the electrophysiological differences between individual iAM clones. Different iAM clones may, for instance, be derived from different parts of the atria (e.g. left or right atrium, epi- or endocardial atrium) or represent different subtypes of atrial myocytes (i.e. nodal, bundle and working cells). Also, the number and location of the chromosomal insertion sites of the LV genomes and the cell's epigenetic status at the moment of immortalization may have contributed to the observed heterogeneity in electrophysiological properties between different iAM clones.

Although single-cell patch-clamp analysis can yield a wealth of information about the electrophysiological behaviour of individual cells and has been widely used to estimate the risk of drug-induced proarrhythmia, the technique does not directly assess proarrhythmic potential and is of limited use for studying arrhythmia mechanisms. Optical mapping, on the other hand, allows investigation of normal and disturbed cardiac electrical impulse propagation in a direct manner with high spatial and temporal resolution^{38,39}. As demonstrated by the experiments described in *Figure 4-6* and *Figure S4, S7-9* (see Supplementary material online), confluent iAM cultures are well-suited for optical mapping studies. In combination with their large proliferation capacity, this opens perspectives for developing high-throughput analyses based on the iAM lines and/or future lines of other cardiomyocytes generated with our conditional immortalization method.

Comparison between HL-1 and iAM-1 cells

Of all AM lines generated to date, the murine AM line HL-1 has the most differentiated phenotype and is therefore most widely used. Side-by-side comparison of the electrophysiological properties of confluent monolayers of differentiated iAM-1 cells and HL-1 cells by optical voltage mapping (*Figure 5* and *Movie III*) showed an average CV for the HL-1 cultures of 1 cm/s, which is about 20-fold lower than that of differentiated iAM-1 cell cultures and in line with previous reports²⁴. Since Ma *et al*⁴⁰ reported a resting membrane potential of -77.7 ± 0.4 mV for HL-1 cells at an extracellular K^+ concentration of 4 mM, the low CV in confluent HL-1 cell monolayers does not seem to result from a high percentage of cardiac fast Na^+ channels being in an inactivated state. The large difference in CV between both cell types thus conceivably relates to the fact that confluent HL-1 monolayers are a blend of proliferating cells without cardiomyocyte functionality, which are electrically coupled to cells that phenotypically resemble embryonic atrial myocytes¹¹. Conversely,

in the iAM cultures at 9 days of differentiation virtually all cells are in a similar advanced stage of differentiation forming a highly conductive cardiac syncytium (*Figure 4, 5* and Supplementary material online, *Figure S4, S5, S7-9*). Gap junctional coupling between undifferentiated and differentiated cells may also explain the apparent discrepancy between the broad optical voltage traces of HL-1 cells in monolayer cultures versus the short APDs recorded for single HL-1 cells following whole-cell current clamping²⁴.

Conclusion

By employing a monopartite LV system allowing inducible expression of the SV40 LT antigen in cardiomyocytes, we have generated lines of iAMs with (functional) properties superior to those of all existing cardiomyocyte lines, none of which yields cells that approach the structural and functional maturity of dox-deprived iAMs. This is especially true for differentiated iAM-1 monolayers, which show homogeneous AP propagation at much higher speeds than obtained with other lines of cardiac muscle cells. The broad applicability of the iAMs was illustrated by their use (i) to study the cardiac ion channel-modulatory activity of toxins and drugs and (ii) as AF model. Since iAMs undergo a highly coordinated and precisely timed cardiomyogenic differentiation process, they might also be ideally suited to study specific aspects of cardiac muscle cell formation and maturation. Finally, because differentiation of iAMs into electrically and mechanically active cardiomyocytes that phenotypically resemble atrial myocytes of newborn rats occurs spontaneously (*i.e.* without the need for complex treatment regimens with expensive [bio]chemicals), iAMs may provide an easy-to-use and cost-effective system to address specific fundamental and applied cardiac research.

Funding

This study received financial support from the Netherlands Heart Institute (ICIN grant 230.148-04 to A.A.F.d.V.), the Royal Netherlands Academy of Arts and Sciences (Chinese Exchange Programme grant 10CDP007 to A.A.F.d.V.), and Ammodo (to D.A.P. and A.A.F.d.V.). Additional support came from the research programme More Knowledge with Fewer Animals (MKMD) with project number 114022503 (to A.A.F.d.V.), which is (partly) financed by the Netherlands Organisation for Health Research and Development (ZonMw) and the Dutch Society for the Replacement of Animal Testing (dsRAT) and from the Chinese Scholarship Council (to J.L.).

Acknowledgements

We thank Brian Bingen, Zeinab Neshati and Iolanda Feola, Niels Harlaar and Annemarie Kip from LUMC's Laboratory of Experimental Cardiology for their help with establishing AM cultures, LV production, generating movie files and RT-qPCR experiments, respectively. We are indebted to Bianca Brundel and Deli Zhang (Department of Physiology, Institute for Cardiovascular Research, VU University Medical Center) for supplying HL-1 cells.

Conflict of interest

None declared.

References

1. Hasenfuss G. Animal models of human cardiovascular disease, heart failure and hypertrophy. *Cardiovasc Res* 1998;**39**:60-76.
2. Robinson N, Souslian L, Gallegos RP, Rivard AL, Dalmaso AP, Bianco RW. *Animal models for cardiac research*. In: Iaizzo PA. Handbook of Cardiac Anatomy, Physiology, and Devices. 3rd ed. Cham: Springer International Publishing, 2015:469-491.
3. Mitcheson JS, Hancox JC, Levi AJ. Cultured adult cardiac myocytes: future applications, culture methods, morphological and electrophysiological properties. *Cardiovasc Res* 1998;**39**:280-300.
4. Parameswaran S, Kumar S, Verma RS, Sharma RK. Cardiomyocyte culture - an update on the in vitro cardiovascular model and future challenges. *Can J Physiol Pharmacol* 2013;**91**:985-998.
5. Spater D, Hansson EM, Zangi L, Chien KR. How to make a cardiomyocyte. *Development* 2014;**141**:4418-4431.
6. Karakikes I, Ameen M, Termglinchan V, Wu JC. Human induced pluripotent stem cell-derived cardiomyocytes: insights into molecular, cellular, and functional phenotypes. *Circ Res* 2015;**117**:80-88.
7. Veerman CC, Kosmidis G, Mummery CL, Casini S, Verkerk AO, Bellin M. Immaturity of human stem-cell-derived cardiomyocytes in culture: fatal flaw or soluble problem? *Stem Cells Dev* 2015;**24**:1035-1052.
8. Herron TJ. Calcium and voltage mapping in hiPSC-CM monolayers. *Cell Calcium* 2016;**59**:84-90.
9. Steinhilber ME, Lanson NA Jr, Dresdner KP, Delcarpio JB, Wit AL, Claycomb WC, Field LJ. Proliferation in vivo and in culture of differentiated adult atrial cardiomyocytes from transgenic mice. *Am J Physiol* 1990;**259**:H1826-1834.
10. Jahn L, Sadoshima J, Greene A, Parker C, Morgan KG, Izumo S. Conditional differentiation of heart- and smooth muscle-derived cells transformed by a temperature-sensitive mutant of SV40 T antigen. *J Cell Sci* 1996;**109** (Pt 2):397-407.
11. Claycomb WC, Lanson NA Jr, Stallworth BS, Egeland DB, Delcarpio JB, Bahinski A, Izzo NJ Jr. HL-1 cells: a cardiac muscle cell line that contracts and retains phenotypic characteristics of the adult cardiomyocyte. *Proc Natl Acad Sci U S A* 1998;**95**:2979-2984.
12. Rybkin II, Markham DW, Yan Z, Bassel-Duby R, Williams RS, Olson EN. Conditional expression of SV40 T-antigen in mouse cardiomyocytes facilitates an inducible switch from proliferation to differentiation. *J Biol Chem* 2003;**278**:15927-15934.
13. Davidson MM, Nesti C, Palenzuela L, Walker WF, Hernandez E, Protas L, Hirano M, Isaac ND. Novel cell lines derived from adult human ventricular cardiomyocytes. *J Mol Cell Cardiol* 2005;**39**:133-147.
14. Goldman BI, Amin KM, Kubo H, Singhal A, Wurzel J. Human myocardial cell lines generated with SV40 temperature-sensitive mutant tsA58. *In Vitro Cell Dev Biol Anim* 2006;**42**:324-331.
15. Zhang Y, Nuglozeh E, Toure F, Schmidt AM, Vunjak-Novakovic G.

- Controllable expansion of primary cardiomyocytes by reversible immortalization. *Hum Gene Ther* 2009;**20**:1687-1696.
16. Lip GY, Fauchier L, Freedman SB, Van Gelder I, Natale A, Gianni C, Nattel S, Potpara T, Rienstra M, Tse HF, Lane DA. Atrial fibrillation. *Nat Rev Dis Primers* 2016;**2**:16016.
 17. Bingen BO, Neshati Z, Askar SF, Kazbanov IV, Ypey DL, Panfilov AV, Schalij MJ, de Vries AA, Pijnappels DA. Atrium-specific Kir3.x determines inducibility, dynamics, and termination of fibrillation by regulating restitution-driven alternans. *Circulation* 2013;**128**:2732-2744.
 18. Feola I, Teplenin A, de Vries AA, Pijnappels DA. Optogenetic engineering of atrial cardiomyocytes. *Methods Mol Biol* 2016;**1408**:319-331.
 19. Bingen BO, Engels MC, Schalij MJ, Jangsangthong W, Neshati Z, Feola I, Ypey DL, Askar SF, Panfilov AV, Pijnappels DA, de Vries AA. Light-induced termination of spiral wave arrhythmias by optogenetic engineering of atrial cardiomyocytes. *Cardiovasc Res* 2014;**104**:194-205.
 20. Szulc J, Wiznerowicz M, Sauvain MO, Trono D, Aebischer P. A versatile tool for conditional gene expression and knockdown. *Nat Methods* 2006;**3**:109-116.
 21. Salva MZ, Himeda CL, Tai PW, Nishiuchi E, Gregorevic P, Allen JM, Finn EE, Nguyen QG, Blankinship MJ, Meuse L, Chamberlain JS, Hauschka SD. Design of tissue-specific regulatory cassettes for high-level rAAV-mediated expression in skeletal and cardiac muscle. *Mol Ther* 2007;**15**:320-329.
 22. Majumder R, Engels MC, de Vries AA, Panfilov AV, Pijnappels DA. Islands of spatially discordant APD alternans underlie arrhythmogenesis by promoting electrotonic dyssynchrony in models of fibrotic rat ventricular myocardium. *Sci Rep* 2016;**6**:24334.
 23. Yu Z, Liu J, van Veldhoven JP, AP IJ, Schalij MJ, Pijnappels DA, Heitman LH, de Vries AA. Allosteric modulation of Kv11.1 (hERG) channels protects against drug-induced ventricular arrhythmias. *Circ Arrhythm Electrophysiol* 2016;**9**:e003439.
 24. Dias P, Desplantez T, El-Harasis MA, Chowdhury RA, Ullrich ND, Cabestrero de Diego A, Peters NS, Severs NJ, MacLeod KT, Dupont E. Characterisation of connexin expression and electrophysiological properties in stable clones of the HL-1 myocyte cell line. *PLoS One* 2014;**9**:e90266.
 25. Lompre AM, Nadal-Ginard B, Mahdavi V. Expression of the cardiac ventricular alpha- and beta-myosin heavy chain genes is developmentally and hormonally regulated. *J Biol Chem* 1984;**259**:6437-6446.
 26. Horváth A, Lemoine MD, Löser A, Mannhardt I, Flenner F, Uzun AU, Neuber C, Breckwoldt K, Hansen A, Girdauskas E, Reichenspurner H, Willems S, Jost N, Wettwer E, Eschenhagen T, Christ T. Low Resting Membrane Potential and Low Inward Rectifier Potassium Currents Are Not Inherent Features of hiPSC-Derived Cardiomyocytes. *Stem Cell Reports*; **10**:822-833.
 27. Dawodu AA, Monti F, Iwashiro K, Schiariti M, Chiavarelli R, Puddu PE. The shape of human atrial action potential accounts for different frequency-related changes in vitro. *Int J Cardiol* 1996;**54**:237-249.
 28. Carmeliet E. Cardiac ionic currents and acute ischemia: from channels to arrhythmias. *Physiol Rev* 1999;**79**:917-1017.

29. Gadsby DC, Nakao M. Steady-state current-voltage relationship of the Na/K pump in guinea pig ventricular myocytes. *J Gen Physiol* 1989;**94**:511-537.
30. Läuger P. Electrogenic ion pumps. 1991.
31. Ypey DL, van Meerwijk WPM, Umar S, Pijnappels DA, Schalij MJ, van der Laarse A. Depolarization-induced automaticity in rat ventricular cardiomyocytes is based on the gating properties of L-type calcium and slow Kv channels. *Eur Biophys J* 2013;**42**:241-255.
32. Itoh H. *Electrophysiological simulation of developmental changes in action potentials of cardiomyocytes*. In: Arjunan SNV, Dhar PK, Tomita, M. E-Cell System: Basic Concepts and Applications. New York: Springer-Verlag, 2013: 75-88.
33. Avila G, Medina IM, Jiménez E, Elizondo G, Aguilar CI. Transforming growth factor- β 1 decreases cardiac muscle L-type Ca^{2+} current and charge movement by acting on the $\text{Ca}_v1.2$ mRNA. *Am J Physiol Heart Circ Physiol* 2007;**292**:H622-H631.
34. Maggio I, Goncalves MA. Genome editing at the crossroads of delivery, specificity, and fidelity. *Trends Biotechnol* 2015;**33**:280-291.
35. Schwach V, Passier R. Generation and purification of human stem cell-derived cardiomyocytes. *Differentiation* 2016;**91**:126-138.
36. Foglia MJ, Poss KD. Building and re-building the heart by cardiomyocyte proliferation. *Development* 2016;**143**:729-740.
37. Uygur A, Lee RT. Mechanisms of Cardiac Regeneration. *Dev Cell* 2016;**36**:362-374.
38. Herron TJ, Lee P, Jalife J. Optical imaging of voltage and calcium in cardiac cells & tissues. *Circ Res* 2012;**110**:609-623.
39. Himel HD IV, Bub G, Lakireddy P, El-Sherif N. Optical imaging of arrhythmias in the cardiomyocyte monolayer. *Heart Rhythm* 2012;**9**:2077-2082.
40. Ma L, Zhang X, Chen H. TWIK-1 two-pore domain potassium channels change ion selectivity and conduct inward leak sodium currents in hypokalemia. *Sci Signal* 2011;**4**:ra37.
41. Loeber G, Tevethia MJ, Schwedes JF, Tegtmeyer P. Temperature-sensitive mutants identify crucial structural regions of simian virus 40 large T antigen. *J Virol* 1989;**63**:4426-4430.
42. Deuschle U, Meyer WK, Thiesen HJ. Tetracycline-reversible silencing of eukaryotic promoters. *Mol Cell Biol* 1995;**15**:1907-1914.

Supporting information

Supplemental methods

Construction of plasmids

DNA constructions were carried out with enzymes from Fermentas (Thermo Fisher Scientific, Breda, the Netherlands) or from New England Biolabs (Bioke', Leiden, the Netherlands) and with oligodeoxyribonucleotides from Eurofins MWG Operon (Ebersberg, Germany) using established procedures or following the instructions provided with specific reagents.

To generate a thermosensitive version of the oncogenic simian virus 40 (SV40) large T (LT) antigen (mutant *tsA58* also known as *tsA438A-V*¹), plasmid pAT153.SV40ori(-)² was incubated with PvuII and the 4.3-kb digestion product was recircularized with bacteriophage T4 DNA ligase to generate pAT153.SV40ori(-).dPvuII. pAT153.SV40ori(-).dPvuII was subsequently cut with HindIII and PvuII and the large digestion product of 4.3 kb was combined with the hybridization product of oligodeoxyribonucleotides 5' CTGTGCTTCTAGAATTATGTGGGGGGAA 3' and 5' AGCTTTCCCCCACATAATTCTAGAAGCACAG 3' (underlined nucleotides represent the mutant LT codon and its complement) producing pAT153.SV40ori(-).dPvuII.LT-*tsA58*. Next, pAT153.SV40ori(-).dPvuII.LT-*tsA58* was linearized with PvuII and the 4.3-kb digestion product was ligated to the 2.0-kb PvuII fragment of pAT153.SV40ori(-) to generate pAT153.SV40ori(-).LT-*tsA58*. pAT153.SV40ori(-).LT-*tsA58* was used as template in a polymerase chain reaction (PCR) with VELOCITY DNA polymerase (GC Biotech, Alphen aan den Rijn, the Netherlands) and primers 5' AGGTTTAAACTACGGGATCCGTGCACCATGGATAAAGTTTTAAACAGAGAGGA 3' and 5' CCGAATTCTTTATGTTTCAGGTCAGGG 3' (underlined nucleotides represent the LT initiation codon and the complement of its termination codon) to amplify the LT-coding sequence. The resulting PCR fragment was inserted into plasmid pJET1.2/blunt using the CloneJET PCR cloning kit (Thermo Fisher Scientific) to generate pJet1.2.LT-*tsA58*. pJet1.2.LT-*tsA58* was incubated with MssI and EcoRI and the 2.5-kb digestion product was combined with the 11.0-kb MssI×EcoRI fragment of lentiviral vector (LV) shuttle plasmid pLV.iMHCK7 to generate pLV.iMHCK7.LT-*tsA58* (Figure 1A). pLV.iMHCK7 is a derivative of pLVET-tTR-KRAB³ (Addgene, Cambridge, MA; plasmid number: 116444) in which the human *EEF1A1* gene promoter and the *Aequorea victoria* enhanced green fluorescent protein (eGFP)-coding sequence were replaced by the striated muscle-specific MHCK7 promoter⁴ and a small polylinker containing unique SpeI, MssI, PstI and EcoRI restriction enzyme recognition sequences.

LV shuttle plasmid pLV.MHCK7.eGFP is a derivative of construct pLV.MHCK7.eYFP.WHVPRE⁵, in which the coding sequence for the *Aequorea victoria* enhanced yellow fluorescent protein and the woodchuck hepatitis virus posttranscriptional regulatory element (WHVPRE) are replaced by the eGFP open reading frame and a mutated shortened version of the WHVPRE designated WHVoPRE⁶.

LV production

To generate vesicular stomatitis virus G protein-pseudotyped particles of LV.iMHCK7.LT-*tsA58*, subconfluent monolayers of 293T cells were transfected with LV shuttle construct pLV.iMHCK7.LT-*tsA58* and the packaging plasmids psPAX2 (Addgene; plasmid number: 12260) and pLP/VSVG (Thermo Fisher Scientific) at a molar ratio of 2:1:1. The 293T cells were cultured in high-glucose Dulbecco's modified Eagle's medium (DMEM; Life Technologies Europe, Bleiswijk, the Netherlands, catalogue number: 41966) with 10% foetal bovine serum (FBS; Life Technologies Europe). The transfection mixture, which consisted of 35 µg of plasmid DNA and 105 µg of polyethyleneimine (Polysciences Europe, Eppelheim, Germany) in 2 ml of 150 mM NaCl per 175-cm² cell culture flask (Greiner Bio-One, Alphen aan den Rijn, the Netherlands), was directly added to the culture medium. The next morning, the transfection medium was replaced by 15 ml of fresh high-glucose DMEM supplemented with 5% FBS and 25 mM HEPES-NaOH (pH 7.4). At ±48 hours after the start of the transfection procedure, the culture supernatants were harvested and cleared from cellular debris by centrifugation at room temperature (RT) for 10 minutes at 3,750×*g* and subsequent filtration through 0.45-µm pore-sized, 33-mm diameter polyethersulfone Millex-HP syringe filters (Millipore, Amsterdam, the Netherlands). To concentrate and purify the LV particles, 30 ml of vector suspension in a 38.5-ml polypropylene ultracentrifuge tube (Beckman Coulter Nederland, Woerden, the Netherlands) was underlayered with 5 ml of 20% (wt/vol) sucrose in phosphate-buffered saline (PBS) and centrifuged for 120 minutes at 4°C with slow acceleration and without braking at 15,000 revolutions per minutes in an SW32 rotor (Beckman Coulter Nederland). Next, the supernatants were discarded and the pellets were suspended in PBS-1% bovine serum albumin (BSA; Sigma-Aldrich, St. Louis, MO) by overnight incubation with gentle shaking at 4°C. The concentrated vector suspension was divided on ice in 50 µl aliquots for storage at -80°C. LV.MHCK7.eGFP particles were generated using the same procedure except for the use of pLV.MHCK7.eGFP instead of pLV.iMHCK7.LT-*tsA58* as LV shuttle plasmid.

Animal experiments

All animal experiments were approved by the Animal Experiments Committee of Leiden University Medical Center and conformed to the Guide for the Care and Use of Laboratory Animals as stated by the US National Institutes of Health.

Isolation and culture of cardiomyocytes

Cardiomyocytes were isolated from neonatal Wistar rat hearts and cultured as detailed elsewhere⁷. Briefly, rats were anaesthetized with 4-5% isoflurane inhalation. After adequate anaesthesia had been confirmed by the absence of pain reflexes, hearts were excised. Atria and ventricles were separated from the hearts, minced and dissociated by 2 subsequent 30-minute treatments with collagenase type I (Worthington Biochemical, Lakewood, NJ) and DNase I (Sigma-Aldrich). Cells were pelleted by centrifugation for 10 minutes at RT and 160×*g* and suspended in Ham's F10 medium (Life Technologies Europe, catalogue number: 11550) supplemented with 100 units/mL of penicillin and 100 µg/mL of streptomycin (Life Technologies Europe) and with 10% heat-inactivated FBS and 10% heat-inactivated horse serum (HS; Life

Technologies Europe). Next, cell suspensions were transferred to Primaria culture dishes (Corning Life Sciences, Amsterdam, the Netherlands) and incubated for 120 minutes at 37°C in a humidified atmosphere of 5% CO₂ to allow preferential attachment of non-cardiomyocytes. The unattached cells (mainly atrial myocytes AMs or ventricle myocytes VMs) were collected, passed through a cell strainer (70-µm mesh pore size; BD Biosciences, Breda, the Netherlands) and seeded at a density of 2×10³ cells/cm² in a 6-well cell culture plate (Corning Life Sciences) coated with fibronectin from bovine plasma (Sigma-Aldrich) for immortalization purposes or on bovine fibronectin-coated glass coverslips in 24-well cell culture plates (Greiner Bio-One) at a density between 2×10⁴ and 8×10⁵ cells/well for comparative studies. LV.iMHCK7.LT-*tsA58*-transduced cells and primary AMs (pAMs) were subsequently maintained in a 1:1 mixture of low-glucose DMEM (Life Technologies Europe, catalogue number: 22320) and Ham's F10 medium (DMEM/F10) supplemented with 5% heat-inactivated HS, 1× penicillin-streptomycin, 2% BSA and sodium ascorbate to a final concentration of 0.4 mM and in DMEM/F10 with 10% heat-inactivated FBS and 100 ng/ml doxycycline (dox) or no dox as indicated, respectively. Culture medium was replaced daily (pAMs and pVMs) or every 2-3 days (immortalized AMs).

For the isolation and culture of neonatal rat ventricular cardiomyocytes (pVMs) the same method was used as for pAMs except that ventricular instead of atrial tissue of newborn rats served as starting material.

HL-1 cells were cultured in 25-cm² cell culture flasks (Corning Life Sciences) for regular passaging and on round glass coverslips (diameter of 15 mm) for optical mapping purposes essentially as described in the MEA Application Note: HL-1 Cardiac Cell Line of Multi Channel Systems (Reutlingen, Germany; http://www.multichannelsystems.com/sites/multichannelsystems.com/files/documents/applications/MEA-Application%20Note_HL-1.pdf).

The best performing line of conditionally immortalized AMs (iAMs) has been designated iAM-1. Inquiries about this cell line and other iAM lines can be sent to iAM-1@hartlongcentrum.nl.

Transduction of pAMs and generation of iAM clones

At day 1 of culture, pAMs were transduced with LV.iMHCK7.LT-*tsA58*. The next day, the inoculum was replaced by culture medium containing 100 ng/ml dox to induce LT expression. The cells were given fresh culture medium every other day. After 1 week of culture, the transduced cells were trypsinized and plated at a low density of 10~20 cells/cm² in a 100-mm diameter cell culture dish (Greiner Bio-One) to generate single-cell clones. After 2-3 weeks, individual cell colonies were picked and expanded in the presence of dox. To investigate their spontaneous cardiomyogenic differentiation ability, iAMs were cultured in the absence of dox for 3, 6, 9 and 12 days and characterized by a combination of molecular biological, cell biological, immunological and electrophysiological techniques.

To facilitate their identification in co-cultures with pAMs, iAM-1 cells were eGFP-labelled using the LV designated LV.MHCK7.eGFP and passaged multiple times in the presence of dox before use as donor cells to avoid carry-over of functional LV.MHCK7.eGFP particles⁸.

Western blotting

Western blotting was carried out as detailed before⁹. After blocking, the membranes were incubated overnight at 4°C with primary mouse monoclonal antibodies directed against LT (1:2,000; Santa Cruz Biotechnology, Dallas, TX, catalogue number: sc-147) or glyceraldehyde 3-phosphate dehydrogenase (GAPDH; loading control; 1:100,000; Millipore, catalogue number: MAB374) and then probed with goat anti-mouse IgG secondary antibodies linked to horseradish peroxidase (1:15,000; Santa Cruz Biotechnology) for 1 hour at RT. Chemiluminescence was produced using the SuperSignal West Femto maximum sensitivity substrate (Thermo Fisher Scientific), captured by a ChemiDoc XRS imaging system (Bio-Rad Laboratories, Veenendaal, the Netherlands) and analysed by Quantity One software (Bio-Rad Laboratories) using the GAPDH signals for normalization purposes.

Immunocytology

Immunostaining of cultured cells was performed as previously described¹⁰ using the following primary antibodies at a dilution of 1:200 in PBS containing 0.1% normal donkey serum (NDS; Sigma-Aldrich): mouse anti-LT (Santa Cruz Biotechnology, catalogue number: sc-147), rabbit anti-Ki-67 (Abcam, Cambridge, United Kingdom, catalogue number: ab15580), mouse anti- α -actinin (Sigma-Aldrich, catalogue number: A7811), rabbit anti-atrial myosin light chain 2 (MLC2a)¹¹ and rabbit anti-connexin 43 (Cx43; Sigma-Aldrich, catalogue number: C6219). Bound antigens were detected using Alexa 488-conjugated donkey anti-rabbit IgG (H+L) (Thermo Fisher Scientific, catalogue number: A21206) and Alexa 568-coupled donkey anti-mouse IgG (H+L) (Thermo Fisher Scientific, catalogue number: A10037). These secondary antibodies were diluted 1:400 in PBS. Hoechst 33342 (10 μ g/ μ l; Thermo Fisher Scientific) was used to counterstain nuclei. Stained cells were visualized using a digital colour camera-equipped fluorescence microscope (Nikon Eclipse 80i; Nikon Instruments Europe, Amstelveen, the Netherlands).

Analysis of cell proliferation and programmed cell death

To assess their proliferation rate, iAMs were cultured at low density in medium with or without 100 ng/ml dox. At different days after culture initiation, cells were collected in PBS, mixed at a ratio of 1:1 with 0.4% Trypan Blue (VWR International, Amsterdam, the Netherlands) in PBS and briefly incubated at RT after which viable cells were counted using a haemocytometer. To distinguish proliferating from non-proliferating cells, monolayer cultures of AMs were immunostained with Ki-67-specific antibodies.

To study apoptosis, cells were incubated with Alexa Fluor-568-conjugated annexin V (Thermo Fisher Scientific, catalogue number: A13202) as described before¹⁰. pAMs treated for 24 hours with 1 μ M of the chemotherapeutic agent doxorubicin (Sigma-Aldrich) served as positive control for the apoptosis assay.

Quantitative analyses of cell surface area, the percentage of Ki-67⁺ cardiomyocytes and cell surface-bound annexin V were performed with the Java-based image processing program Image J (version 1.50i, National Institutes of Health, Bethesda, MD).

Reverse transcription-quantitative PCR (RT-qPCR)

RT-qPCR was performed as previously reported¹⁰. Briefly, iAMs were seeded at a density of 8×10^5 cells/well in 24-well cell culture plates and cultured for 1 day in medium containing 100 ng/ml dox. The next day, cells were either lysed in TRIzol Reagent (Thermo Fisher Scientific) and total RNA was isolated using the RNeasy Mini kit (QIAGEN Benelux, Venlo, the Netherlands) or kept for 3, 6, 9 or 12 days in culture medium without dox prior to cell lysis and RNA extraction. The RNA was reverse transcribed with the iScript cDNA synthesis kit (Bio-Rad Laboratories) and gene expression levels were determined by PCR using the Bioline SensiFAST SYBR No-ROX kit (GC biotech) and intron-spanning primer pairs (*Table S1*). Due to the high nucleotide sequence identity of the pacemaker channel genes, *Hcn2* and *Hcn4* mRNA levels were determined using TaqMan primer/probe sets Rn01408572_mH and Rn00572232_m1), respectively, together with TaqMan Universal Master Mix II (all from Thermo Fisher Scientific). PCR amplifications were performed in a CFX96 Touch Real-Time PCR Detection System (Bio-Rad Laboratories) or in a QuantStudio 5 Real-Time PCR System (Thermo Fisher Scientific). Per target gene 3 independent experiments were performed consisting of 3 samples per experiment. Quantitative analyses were based on the $2^{-\Delta\Delta CT}$ method using CFX Manager software (Bio-Rad Laboratories). PCR amplifications of the rat 18S rRNA gene (*Rn18s*) were included for normalization purposes.

Optical voltage mapping

For studying action potential (AP) propagation in confluent monolayer cultures, cells were seeded at a density of 8×10^5 cells/well in 24-well cell culture plates onto bovine fibronectin-coated round glass coverslips (diameter of 15 mm) and subjected to optical voltage mapping using di-4-ANEPPS (Thermo Fisher Scientific) as fluorescent voltage indicator as described previously⁵. The measurements were carried out at 37°C on 9-day-old pAM and pVM cultures and on iAMs that had been maintained for 0, 3, 6, 9 and 12 days in dox-free medium. Optical signals were captured using a MiCAM ULTIMA-L imaging system (SciMedia, Costa Mesa, CA). Optical traces were analysed using Brain Vision Analyzer 1208 software (Brainvision, Tokyo, Japan). To minimize noise artefacts, calculations were based on the average of the signals at a selected pixel and its eight nearest neighbours. Conduction velocity (CV) and AP duration (APD) at different percentages of repolarization were determined using cardiomyocyte cultures showing uniform AP propagation and 1:1 capture after 1-Hz local electrical stimulation with an epoxy-coated bipolar platinum electrode delivering square 10-ms, 8-V suprathreshold electrical impulses via a STG 2004 stimulus generator and MC Stimulus II software (both from Multi Channel Systems). Burst pacing with a cycle length of 20-100 ms was used to induce reentry. The effects of tertiapin (100 nM, Alomone Labs), astemizole (100 nM, a gift of Zhiyi Yu), carbachol (2 μ M, Alcon, Gorinchem, the Netherlands) and ouabain (100 -400 μ M, Sigma-Aldrich) were investigated by pipetting them directly into the medium and dispersing them by gentle shaking, followed by optical mapping. To facilitate APD comparison, the amplitude of the optical signal traces was normalized for all samples within a given experiment.

Patch-clamping

Whole-cell patch-clamp recordings were conducted on single iAMs and pAMs (2.5×10^4 cells/ 2-cm^2 well) and on iAM and pAM monolayers (8×10^5 cells/ 2-cm^2 well) seeded on fibronectin-coated glass coverslips. The monolayer measurements were carried out using 9-day-old cultures of freshly isolated pAMs or iAMs that were cultured for 9 days in the absence of dox. For single-cell measurements, freshly isolated pAMs were cultured for 2-3 days before patch-clamping. Single-cell patch-clamping of iAMs was done 1-3 days after low-density replating of monolayer cells that had been maintained for 8-9 days without dox unless indicated otherwise. For patch-clamp experiments, pAMs and iAMs were submerged in a Tyrode bath solution containing (in mM): 126 NaCl, 11 glucose, 10 HEPES, 5.4 KCl, 1 MgCl₂, and 1.8 CaCl₂ (adjusted to pH 7.40 with NaOH). Patch recordings were conducted 15-60 minutes later at 20-23°C. Data acquisition was done using an inverted Zeiss Axiovert 35 microscope (Carl Zeiss, Oberkochen, Germany), an MPC-200 multi-micromanipulator system (Sutter Instrument, Novato, CA) and a conventional patch-clamp rig consisting of a CV-7B head stage, MultiClamp 700B amplifier and a Digidata 1440A A/D converter (Axon CNS, Molecular Devices, Sunnyvale, CA). Patch pipettes were fabricated from borosilicate glass capillaries with an inner and outer diameter of 1.17 and 1.5 mm, respectively (Harvard Apparatus, Kent, United Kingdom), using a vertical puller (P-30; Sutter Instrument). Pipette tips were fire-polished and had typical tip resistances for single cell and monolayer measurements of 2-4 and 4-7 MΩ, respectively, when filled with a solution containing (in mM): 80 potassium DL-aspartate, 40 KCl, 8 NaCl, 5.5 glucose, 5 HEPES, 5 EGTA, 1 MgCl₂, 4 Mg-ATP, and 0.1 Na₃-GTP (adjusted to pH 7.20 with KOH). The plasma membrane resistance (R_m) of single pAMs and iAMs at their resting membrane potential (RMP) was approximately 1.1 and 0.9 GΩ, respectively. The effects of carbachol (2 μM) and ouabain (100 and 300 μM) were investigated via local drug perfusion while continuously monitoring the RMP. For fast Na⁺ current analysis, signals induced by 50-ms depolarizing pulses in 10-mV increments starting from a holding potential of -80 mV in the absence and presence of 10 μM tetrodotoxin (TTX, Alomone Labs, Jerusalem, Israel) were digitally subtracted. Voltage clamp recordings were ≥75% compensated for pipette series resistance and capacitive transients. Throughout the experiments, the current and voltage outputs of the amplifier were continuously sampled at 10 kHz after low-pass filtered at 4 kHz with a four-pole Bessel filter. Data acquisition was carried out using pCLAMP 10.7 software (Axon CNS, Molecular Devices).

Current densities were determined by normalizing peak current amplitudes to cell capacitance. Voltage dependence of activation was analysed by fitting the data with a single Boltzmann equation, $I = I_{max} / (1 + e^{-\frac{V-V_{1/2}}{k}})$, where V is the variable test potential, $V_{1/2}$ the voltage of half-maximum activation, k the slope factor, and I_{max} the normalized maximum amplitude of the Na⁺ current. All data were corrected for liquid junction potentials. Data analysis was done using Clampfit 10.7 (Axon CNS, Molecular Devices), Excel (version 2010, Microsoft, Redmond, WA) and Prism 7 (Graphpad Software, La Jolla, CA).

Atrial tissue culture and iAM injection in cultured atrial tissue

Atrial tissue from neonatal rats was used as graft recipient of iAMs. Two-day-old Wistar rats were anaesthetized by 4-5% isoflurane inhalation and adequate anaesthesia was confirmed by the absence of reflexes. After the chest was opened and the inferior vena cava was cut off with scissors, the right atrium was punctured with a 19-gauge needle. The heart was perfused through this needle with pre-warmed and oxygenated PBS containing 10 IU/ml heparin (LEO Pharma, Amsterdam, the Netherlands) to flush out the blood. Two and a half μl of growth factor-reduced Matrigel (BD Biosciences) was mixed with 2.5 μl cell suspension containing 5×10^4 iAMs and injected into the bilateral atrial free walls using a 25- μl syringe equipped with a 33-gauge needle (Hamilton Robotics, Reno, NV).

Subsequently, the atrial tissue including the injected area was excised and cultured with the following modifications. The atrial tissue was placed with the endocardial surface down onto the semi-porous polytetrafluoroethylene membrane (0.4 μm pore size) of a PICM0RG50 cell culture insert (Millipore) in a 35-mm diameter Petri dish containing 1 ml sterilized Tyrode's solution (TS; 136 mM NaCl, 5.4 mM KCl, 10 mM MgH_2PO_4 , 1 mM MgH_2PO_4 , 10 mM glucose, 0.9 mM CaCl_2) of RT and gradually warmed to 37°C. Next, the TS was replaced with 1 ml pre-warmed low-glucose DMEM supplemented with 1% heat-inactivated FBS, 1 \times penicillin-streptomycin, 1 \times B-27 supplement minus antioxidants (Life Technologies Europe) and 5 μM Z-Asp-2,6-dichlorobenzoyloxymethylketone (Santa Cruz Biotechnology) and the tissue was kept at 37°C in humidified 95% air-5% CO_2 (culture conditions) until histological examination. Culture medium was replaced every 2 days.

Whole tissue staining and confocal microscopy

Neonatal rat atrial tissue was quickly washed 3 times with PBS and fixed by incubation for 30 minutes at 4°C in buffered 4% formaldehyde (Added Pharma, Oss, the Netherlands) followed by 3 quick washes with PBS and a 5-minute wash with PBST (0.1% Triton X-100 Sigma-Aldrich in PBS). Next, aspecific binding sites were blocked by incubation for 1 hour at RT with 10% NDS in PBST. After two 10-minute washes with PBST, samples were incubated overnight at 4°C with primary antibodies directed against sarcomeric α -actinin to detect cardiomyocytes (mouse IgG1, clone EA-53; Sigma-Aldrich) or against eGFP to detect iAMs (rabbit IgG, polyclonal; Thermo Fisher Scientific, catalogue number: A11122) and diluted 1:200 in PBS-1% FBS. After 3 quick and four 15-minute washes with PBS, the tissues were incubated with appropriate Alexa Fluor 488/568-conjugated secondary antibodies of donkey origin (1:200 dilution in PBS containing 1% FBS) for 4 hours at 4°C followed by another sequence of 3 short and 4 long washes with PBS. Nuclear counterstaining was performed by incubating the cells for 10 minutes at RT with 10 $\mu\text{g}/\text{ml}$ Hoechst 33342 followed by 3 washes with PBS. Coverslips were mounted in Vectashield mounting medium (Vector Laboratories, Burlingame, CA). Images were acquired with a Leica TCS SP8 confocal laser scanning microscope (Leica Microsystems, Rijswijk, the Netherlands). For Z plane reconstruction, we acquired confocal stacks with a step size of 0.3 μm and analysed the resulting images using Leica Application Suite AF Lite software (Leica Microsystems).

Plasmid DNA transfection of iAMs.

For monitoring the transfection efficiency of iAMs with plasmid DNA, we used the eGFP-encoding mammalian expression plasmid pU.CAG.eGFP. One day before transfection, iAMs were seeded at a density of 4.8×10^5 cells per well in a 24-well cell culture plate and maintained in iAM culture medium with dox. The next day, the cells were transfected with Lipofectamine 3000 reagent (Thermo Fisher Scientific) according to the manufacturer's instructions. To this end, 50 μ l of plasmid DNA-lipid complexes containing 500 ng of pU.CAG.eGFP DNA, 1 μ l of P3000 reagent and 1.5 μ l of Lipofectamine 3000 reagent diluted in Opti-MEM I reduced serum medium (Thermo Fisher Scientific) were added per well to 500 μ l of iAM culture medium without dox. At the indicated times after the start of the transfection procedure, the cells were processed for flow cytometry using a BD Accuri flow cytometer (BD Biosciences), (immuno)fluorescence microscopy and optical voltage mapping. For the cells that were analysed at day 9 post-transfection, the transfection medium was replaced with regular iAM culture medium without dox 2 days after the addition of the lipoplexes.

Statistical analyses

Data were derived from a specified number (N) of observations from 3 different cell cultures. Unless otherwise stated, data were expressed as mean \pm standard deviation (SD) and SDs were represented by error bars. All data were analysed with the nested ANOVA test using the Real Statistics Resource Pack software (release 5.1, copyright 2013 – 2017, Charles Zaiontz, www.real-statistics.com). For comparisons involving >2 experimental groups, this test was followed by Bonferroni *post-hoc* analysis. Results were considered statistically significant at P values <0.05 . Statistical significance was expressed as follows: *: $P < 0.05$, **: $P < 0.01$, ***: $P < 0.001$, ****: $P < 0.0001$.

Supplemental results

Excitability of iAMs

Short depolarizing current-clamp stimulations of single cells (10-20 ms, 100-300 pA, holding potential: -80 mV) were sufficient to evoke APs in pAMs (*Figure S2B*, left panel) and in a fraction of iAMs (*Figure S2B*, right panel). The fraction of these so-called excitable iAMs gradually increased from $\pm 35\%$ at day 3 of culture in the absence of dox to $\pm 90\%$ at day 9 and 12 after the initiation of the differentiation process by dox removal (*Figure S2C*).

The shapes of the pAM and iAM APs were similar based on the nearly identical APDs at 30 and 80% repolarization (APD₃₀ and APD₈₀, respectively). Also, while the AP amplitudes of iAMs did not significantly differ from those of pAMs although iAMs had a smaller upstroke velocity and overshoot than pAMs (*Table S3*). Thus, overall, the excitability properties of pAMs and cardiomyogenically differentiated iAMs were rather similar.

To investigate the ionic basis of the APs generated by iAMs, whole-cell membrane current was recorded using voltage steps applied from a holding potential of -90 mV to test potentials ranging from -130 through +70 mV. In pAMs (*Figure S2B*, left panel), the whole-cell current evoked by hyperpolarizing potentials was

inward and stationary and had the properties of an inward rectifier K^+ current¹². The magnitude of this current gradually declined to zero when increasing the potentials from -130 to -70 mV. Depolarization beyond a holding potential of -70 mV elicited a large, fast transient inward current with a time course typical of a fast voltage-activated Na^+ current, as in Ramos-Mondragon *et al.*¹³, and consistent with mRNA expression of *Scn5a* (Figure S1A). Upon further depolarization, the fast inward current became smaller and gradually gave way to a tiny outward current which, based on its electrophysiological characteristics and the RT-qPCR data, likely represents an outward rectifier K^+ current. As shown in the right panel of Figure S2B, excitable iAMs displayed a similar total inward current as pAMs but a much stronger total outward current and no obvious inwardly rectifying K^+ current (*i.e.* I_{K1}), consistent with the absence of detectable *Kcnj2* expression in iAMs (Figure S1H). Since I_{K1} is important for maintaining a stable negative RMP¹², optical voltage mapping and patch-clamp studies were conducted to determine the role of the atrium-specific acetylcholine-activated K^+ channels (*i.e.* $K_{ir3.1}$ and $K_{ir3.4}$) and the electrogenic Na^+/K^+ pump in regulating the RMP of cardiomyogenically differentiated iAMs (Figure S3).

First, we applied the muscarinic receptor agonist carbachol to maximize $I_{K,ACH}$ currents in confluent pAM and cardiomyogenically differentiated iAM monolayers. Carbachol had no effect on the CV (Figure S3A and D) or RMP of the iAM (-67.5 ± 2.5 mV vs -67.1 ± 2.6 mV in control cultures, $N=8$) and pAM (-64.5 ± 1.9 mV vs -64.3 ± 1.7 mV, $N=7$) monolayers (Figure S3B and E). Also, no carbachol effect was measured in single pAMs (Figure S3F). However, iAMs dissociated from cardiomyogenically differentiated monolayers and subsequently cultured as single cells for 1-3 days showed a hyperpolarizing shift of -16.9 ± 2.6 mV in the RMP after carbachol administration (Figure S3C), thereby approaching the RMP of pAMs.

To determine the role of the Na^+/K^+ ATPase in maintaining a hyperpolarized RMP, its activity was inhibited in a graded manner by exposing pAM and cardiomyogenically differentiated iAM monolayers to increasing concentrations of ouabain. After ouabain administration, the CV decreased dose-dependently in both the pAM and iAM monolayers, although the iAM cultures seemed somewhat more sensitive to ouabain than the pAM cultures. Also, monolayers subjected to 300 and 400 μM ouabain showed partial or full conduction block in optical mapping experiments (Figure S3G and J). These findings are consistent with the patch-clamp results, which showed a dose-dependent depolarizing effect of ouabain on the RMP of the monolayers (Figure S3H, I, K and L) due to both electrogenic effects and changes in the intracellular ion concentrations. To specifically investigate the electrogenic effects of the Na^+/K^+ pump, we performed single-cell patch-clamp measurements, because in these experiments the intra- and extracellular ion concentrations are fixed by the composition of the pipette and bath solutions, respectively. Since this gave a similar depolarizing effect of ouabain on the RMPs of pAMs and iAMs as found in the monolayer studies, we conclude that the Na^+/K^+ pump plays an important electrogenic role in maintaining a negative RMP in iAMs as well as pAMs. This result explains why iAM monolayers despite the lack of detectable *Kcnj2* expression (Figure S1H) are able to generate a stable hyperpolarized RMP to maintain excitability. Furthermore, the RMPs of single iAMs are less stable and more vulnerable to the

measurement conditions of the whole-cell patch-clamp (*Figure S2A*)¹⁴, but are easily repolarized by (full) activation of $K_{ir3.x}$ channels.

In conclusion, the electrogenic contribution of the Na^+/K^+ pump to their RMP allows iAMs to display similar excitability properties as pAMs linked to the presence of similarly strong voltage-activated Na^+ currents.

iAMs as *in vitro* model for studying ion channel-drug interactions

Drug-induced ventricular arrhythmias due to inadvertent blockade of the $K_v11.1$ channel represents a major safety concern in drug development¹⁵. RT-qPCR analysis showed that the *Kcnh2/K_v11.1* gene is highly expressed in iAMs peaking at 6 days after the initiation of differentiation. At this time, *Kcnh2* transcripts were 16-fold more abundant in iAMs than in pAMs at culture day 9 (N=3, $P<0.01$; *Figure S1G*). Double immunostaining of these cells for $K_v11.1$ and sarcomeric α -actinin showed that both cell types expressed the $K_v11.1$ protein and that it was concentrated around the nucleus and at the sarcolemma (*Figure S8A*). To test whether iAMs could be used to identify unintended $K_v11.1$ blockers, the effect of exposing iAMs at day 6 of differentiation to 100 nM of the antihistamine astemizole, which was previously shown to efficiently and selectively block the $K_v11.1$ channel¹⁶, was studied by optical voltage mapping. Astemizole significantly increased APD at 40 and 90% repolarization (APD₄₀ and APD₉₀, respectively) from 21.5 ± 1.0 and 88.7 ± 5.4 ms in vehicle-treated cultures to 30.2 ± 2.1 and 110.9 ± 4.2 ms in cultures containing 100 nM astemizole (N=6, $P<0.01$; *Figure S8B and C*) without affecting CV (14.8 ± 2.8 cm/s vs 14.5 ± 1.1 cm/s in control cultures; N=6, $P=0.57$; *Figure S8D and E*). These data demonstrate the presence of a detectable I_{Kr} in differentiating iAMs and show the utility of AM cultures as *in vitro* model to investigate the AP-prolonging effects of $K_v11.1$ blockers.

Plasmid DNA transfection of iAMs

The practical applicability of iAMs would benefit greatly from them being well transfectable with plasmid DNA. We hence tested whether iAMs would be amenable to plasmid DNA transfection with Lipofectamine 3000. Near-confluent cultures of proliferating iAMs were lipofected with the eGFP-encoding mammalian expression plasmid pU.CAG.eGFP in dox-free medium and transgene expression was assessed by direct fluorescence microscopy and flow cytometry at 2 and 9 days after dox removal (*Figure S9A and B*). At 2 days post-transfection, approximately 50% of the iAMs were eGFP⁺, which percentage did not decrease following incubation of the cells in dox-free medium for 7 more days. Importantly, transfected cells differentiated equally well into functional cardiomyocytes as their non-transduced counterparts judged from the results of α -actinin immunostaining (*Figure S9C*) and optical voltage mapping (*Figure S9D*) of the iAM cultures at 9 day after transfection.

Engraftment of iAMs into viable neonatal rat atrium

To investigate their ability of engraftment, we developed a transplantation model to study the engraftment of iAMs in neonatal rat atrium (*Figure S10A*). eGFP-labelled iAMs were cultured for 2 days in dox-free medium to initiate cardiomyogenic differentiation and subsequently injected into the atrium. Following iAM injection, the

atrium was excised and kept in culture for 6 days. The presence of spontaneous contractions at the end of the culture period demonstrated that the atrial tissue was still viable after 6 days of culture (Supplementary material online, *Movie V*). Confocal laser scanning microscopy of the tissue after fixation at the end of the culture period revealed the presence of eGFP⁺ cells throughout the atrium (*Figure S10B*). Immunostaining for α -actinin showed that many of the eGFP⁺ cells possessed highly organized sarcomeres (*Figure S10B*), whose length (*i.e.* distance between 2 Z-lines) did not significantly differ from that of pAMs (*Figure S10C*). Collectively, these data provide evidence for the cardiomyogenic differentiation and structural integration of transplanted iAMs into atrial tissue.

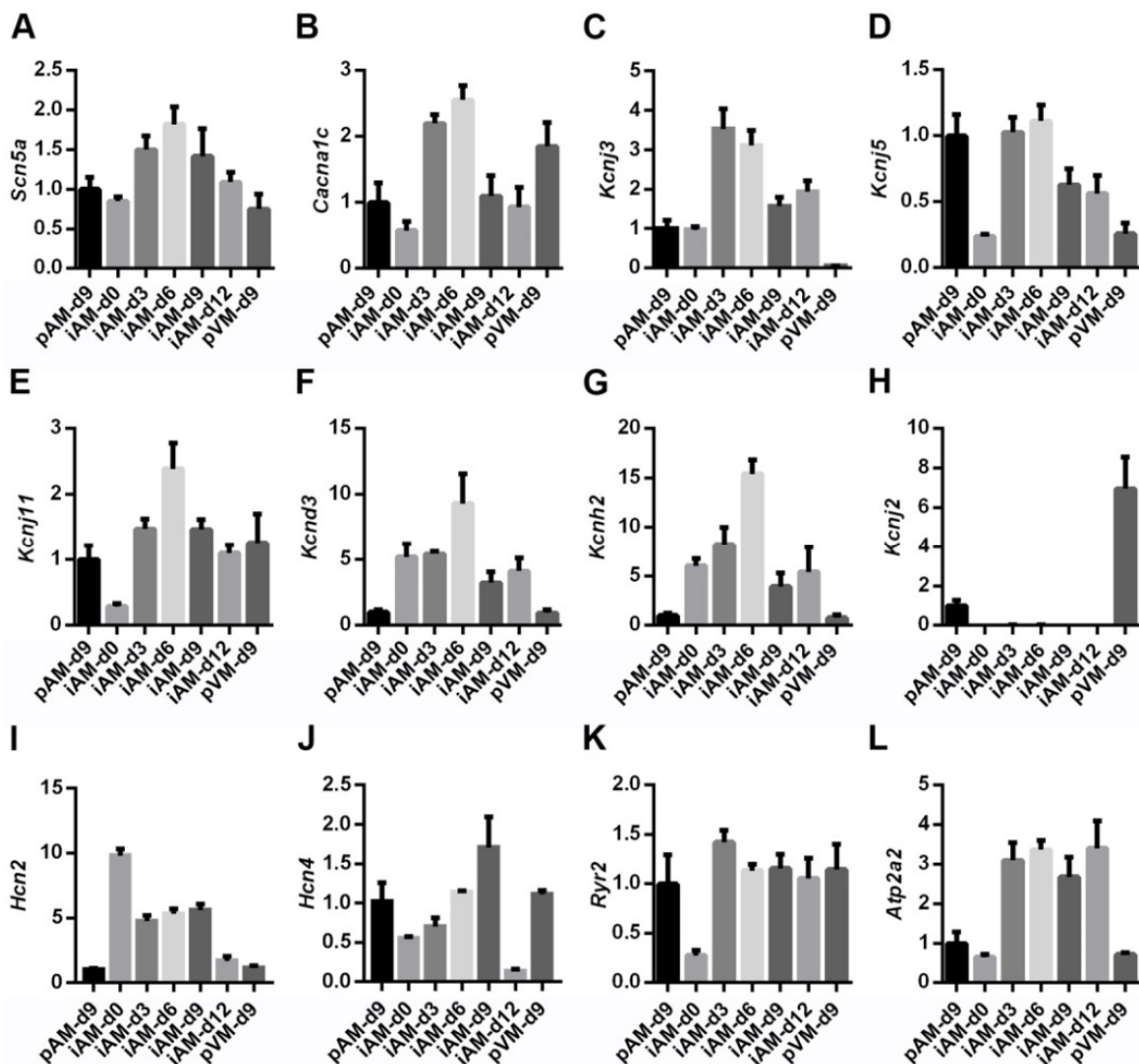


Figure S1. Analysis by RT-qPCR of the expression of the cardiac ion channel genes *Scn5a* (A), *Cacna1c* (B), *Kcnj3* (C), *Kcnj5* (D), *Kcnj11* (E), *Kcnd3* (F), *Kcnh2* (G), *Kcnj2* (H), *Hcn2* (I) and *Hcn4* (J) and the cardiac Ca²⁺-handling protein genes *Ryr2* (K) and *Atp2a2* (L) in pAMs and pVMs at day 9 of culture and in iAMs on the indicated days of differentiation. mRNA levels are expressed relative to those in 9-day-old pAM (pAM-d9) cultures, which were set at 1. Data are presented as mean±SD, N=3 individual preparations.

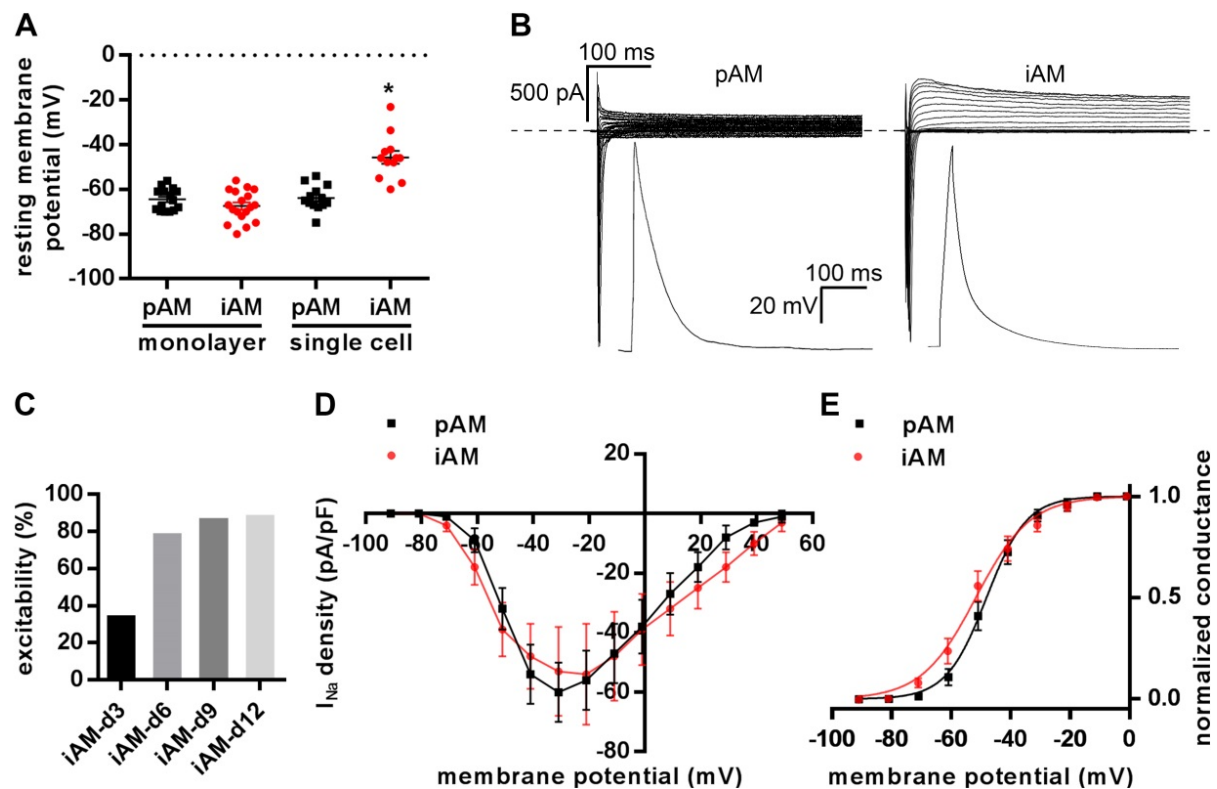


Figure S2. Single-cell patch-clamp analysis of pAMs and cardiomyogenically differentiated iAMs. (A) RMP of pAM monolayers (-64.5 ± 1.2 mV, $N=15$), iAM monolayers (-67.5 ± 1.6 mV, $N=18$), single pAMs (-63.9 ± 1.5 mV, $N=13$) and single iAMs (-45.7 ± 2.9 mV, $N=12$). (B) Whole-cell membrane current traces and APs of a pAM at culture day 3 (left) and an iAM kept in the absence of dox for 12 days (right). Before starting the measurement, the cells were clamped at a holding potential of -80 mV. (C) Graph showing the percentage of excitable iaCMCs at 3, 6, 9 and 12 days of differentiation. $N=9, 9, 7$ and 8 for iaCMC-d3, iaCMC-d6, iaCMC-d9 and iaCMC-d12, respectively. (D) $Na_v1.5$ I-V relationship and I_{Na} current (*i.e.* TTX-sensitive current) densities in single pAMs and iAMs. Current density was obtained by normalizing peak Na^+ currents to cell capacitance. (E) Steady-state of $Na_v1.5$ activation. pAM $V_{1/2} = -48.2 \pm 2.4$ mV, slope factor $= 6.8 \pm 1.0$ ($N=5$); iAM $V_{1/2} = -51.7 \pm 2.5$ mV, slope factor $= 9.1 \pm 1.1$ ($N=6$). Peak current densities and steady-state activation of single pAMs and iAMs were similar. Data are presented as mean \pm SEM. Statistics was done using the nested ANOVA test. $*P < 0.05$.

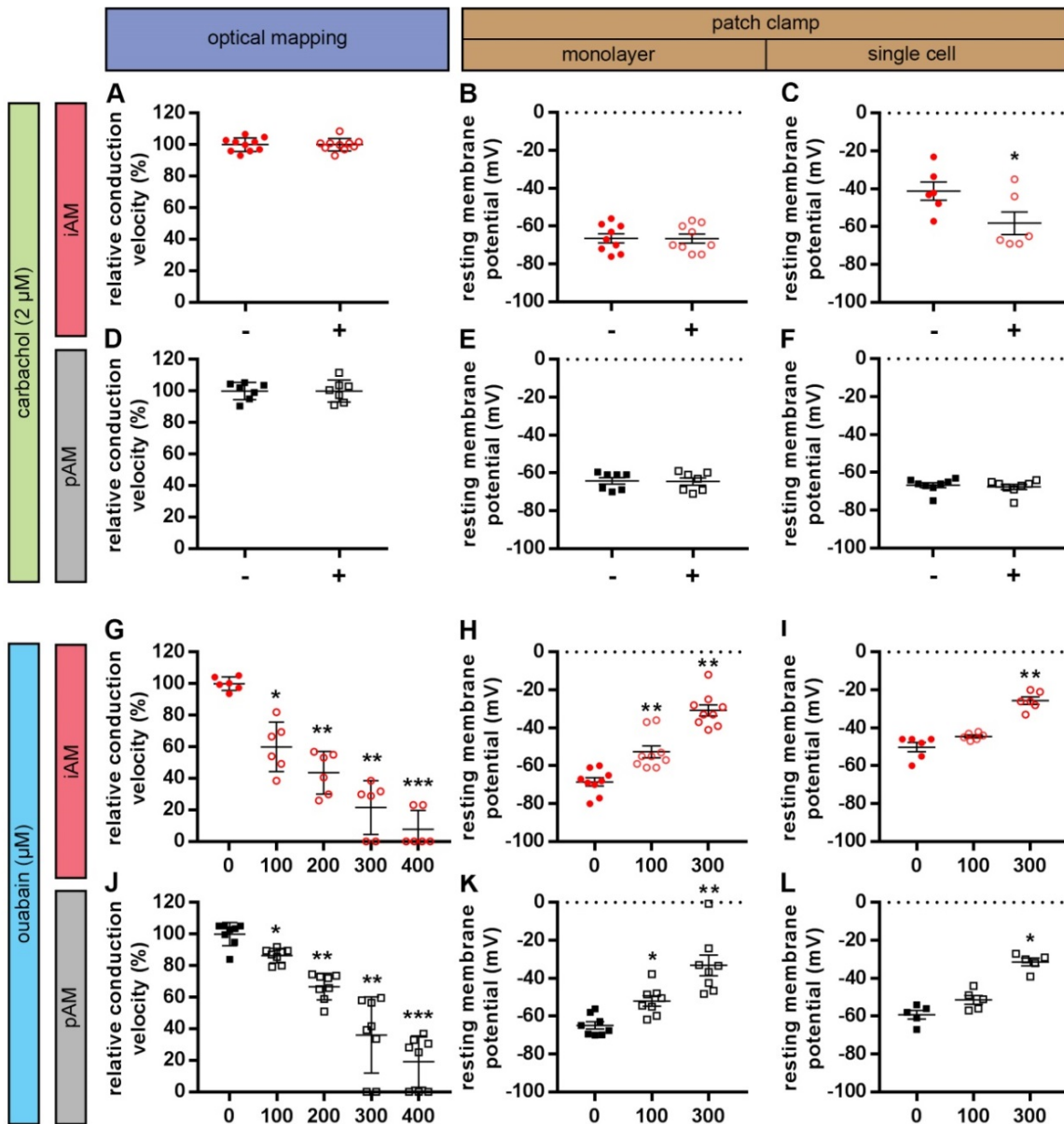


Figure S3. Electrophysiological analyses of pAM and iAM monolayers and single cells using optical voltage mapping and whole-cell patch-clamp recordings. Administration of 2 μM of carbachol to 9-day-old pAM monolayers and cardiomyogenically differentiated iAM monolayers did not affect the CV of (A) iAM (N=10) and (D) pAM monolayers (N=7). Consistently, patch-clamp recordings showed no shift in the RMP of (B) iAM (N=9) and (E) pAM (N=7) monolayers after carbachol treatment. Also carbachol had no effect on the RMP of single 2-3 day-old pAMs (N=8). However, iAMs dissociated from monolayers that had maintained for 9 days in the absence of dox showed a significant shift in the RMP (-16.9 ± 2.6 mV, N=6) towards more negative potentials upon exposure to 2 μM carbachol. Statistics was done using the nested ANOVA test. Analysis by optical voltage mapping and whole-cell patch-clamp of cardiomyogenically differentiated iAM monolayers (G, N=6; and H, N=9) and single cells (I, N=6), as well as pAM monolayers (J, N=8; and K, N=8) and single cells (L, N=5) subjected to increasing concentrations of ouabain showed a significant dose-dependent decrease in CV and a depolarization of the RMP. Thus, the Na^+/K^+ ATPase plays a crucial role in maintaining a stable negative RMP in both pAMs and iAMs. Statistics was done using the nested ANOVA test with Bonferroni *post-hoc* correction. Optical voltage mapping data are presented as mean \pm SD, patch-clamp data as mean \pm SEM. * $P < 0.05$, ** $P < 0.01$ and *** $P < 0.001$.

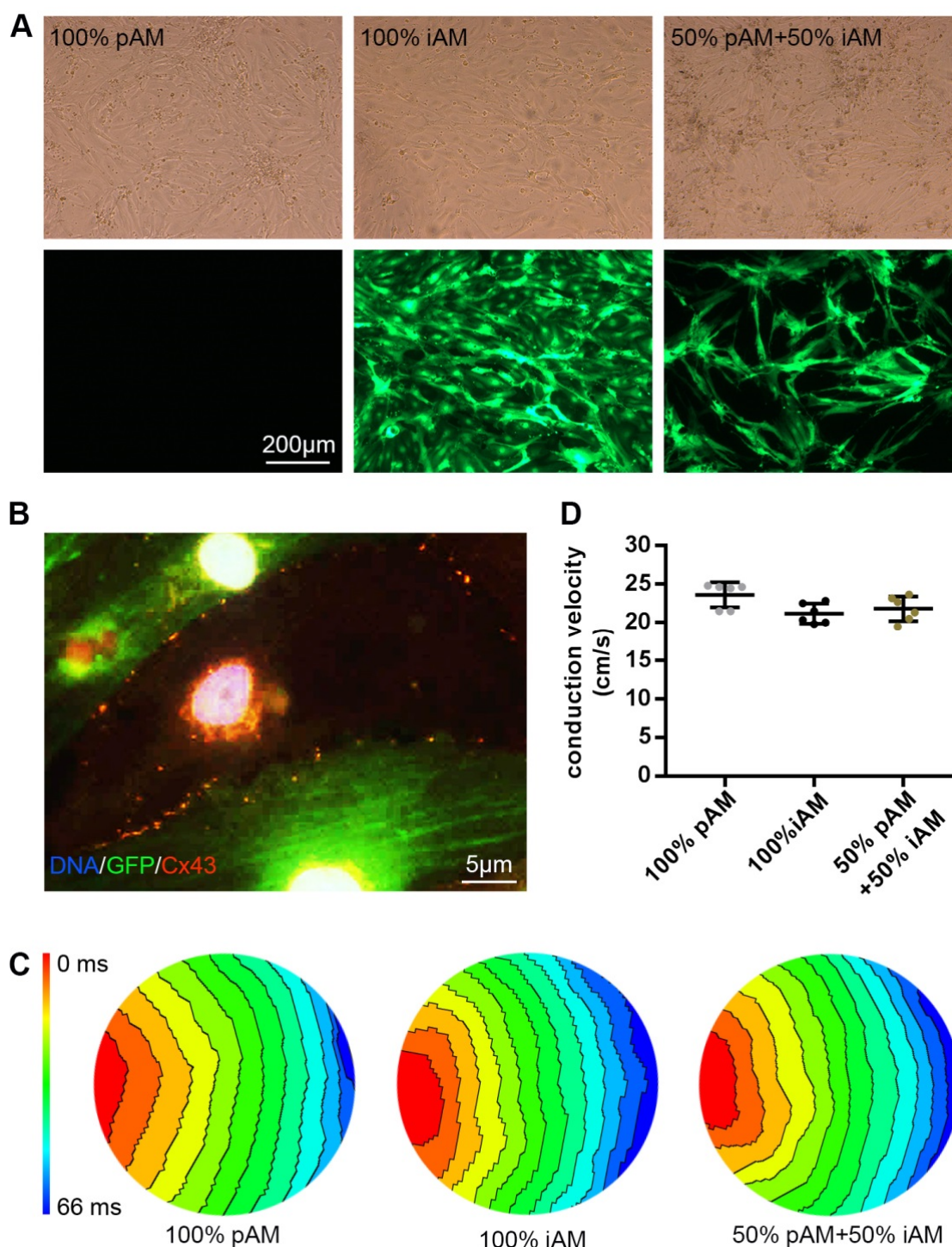


Figure S4. Comparison by optical voltage mapping and 1-Hz electrical point stimulation of the electrophysiological properties of confluent 9-day-old cultures of pAMs, dox-deprived eGFP-labelled iAMs (eGFP-iAMs) and 50% pAMs-50% eGFP-iAMs. (A) Bright field images (upper panel) and fluorescence images (lower panel) of each culture type. (B) Fluorescence image of 9-day-old pAM/eGFP-iAM co-culture immunostained for Cx43 (red) showing its presence at interfaces between iAMs (green) and pAMs. Cell nuclei have been visualized by staining with Hoechst 33342 (blue). (C, D) Activation maps (C; isochrones are separated by 6 ms) and CV quantification (D) reveal no significant different in the speed of AP propagation between the 3 culture types. Data are presented as mean \pm SD, N=6 cell cultures per group from 3 individual preparations. Statistics was done using the nested ANOVA test with Bonferroni *post-hoc* correction.

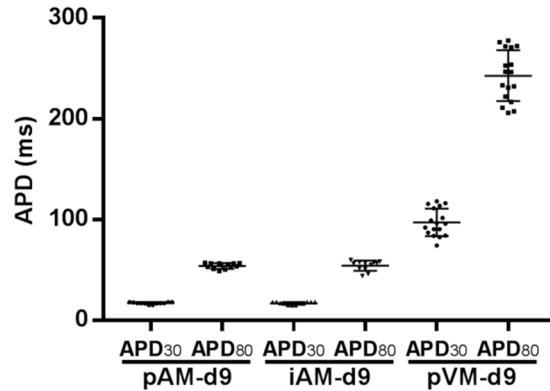


Figure S5. Comparison by optical voltage mapping and 1-Hz electrical point stimulation of APD₃₀ and APD₈₀ of pAMs and pVMs in 9-day-old cultures with those of iAMs at day 9 of differentiation showing that the pVMs have much longer APDs than the atrial myocytes. Data are presented as mean±SD, N=12 cell cultures per group from 4 individual preparations.

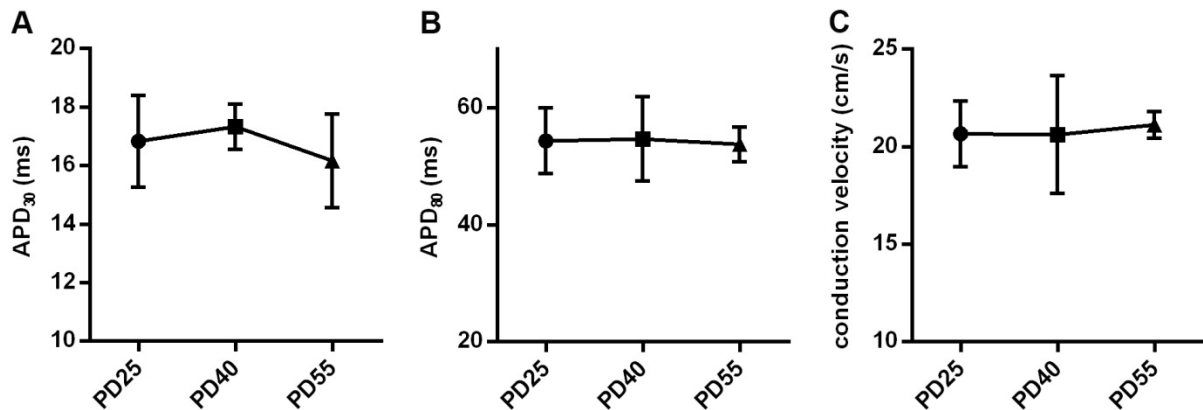


Figure S6. Comparison by optical voltage mapping and 1-Hz electrical point stimulation of the electrophysiological properties of iAMs at day 9 of differentiation (iAM-d9) that, after being cryopreserved, went through 25, 40 or 55 passage doublings (PDs) prior to dox removal. CV (A), APD₃₀ (B) and APD₈₀ (C) did not significantly differ between iAM-d9 of different PD. Data are presented as mean±SD, N=12 cell cultures per group from 4 individual preparations. Statistics was done using the nested ANOVA test with Bonferroni *post-hoc* correction.

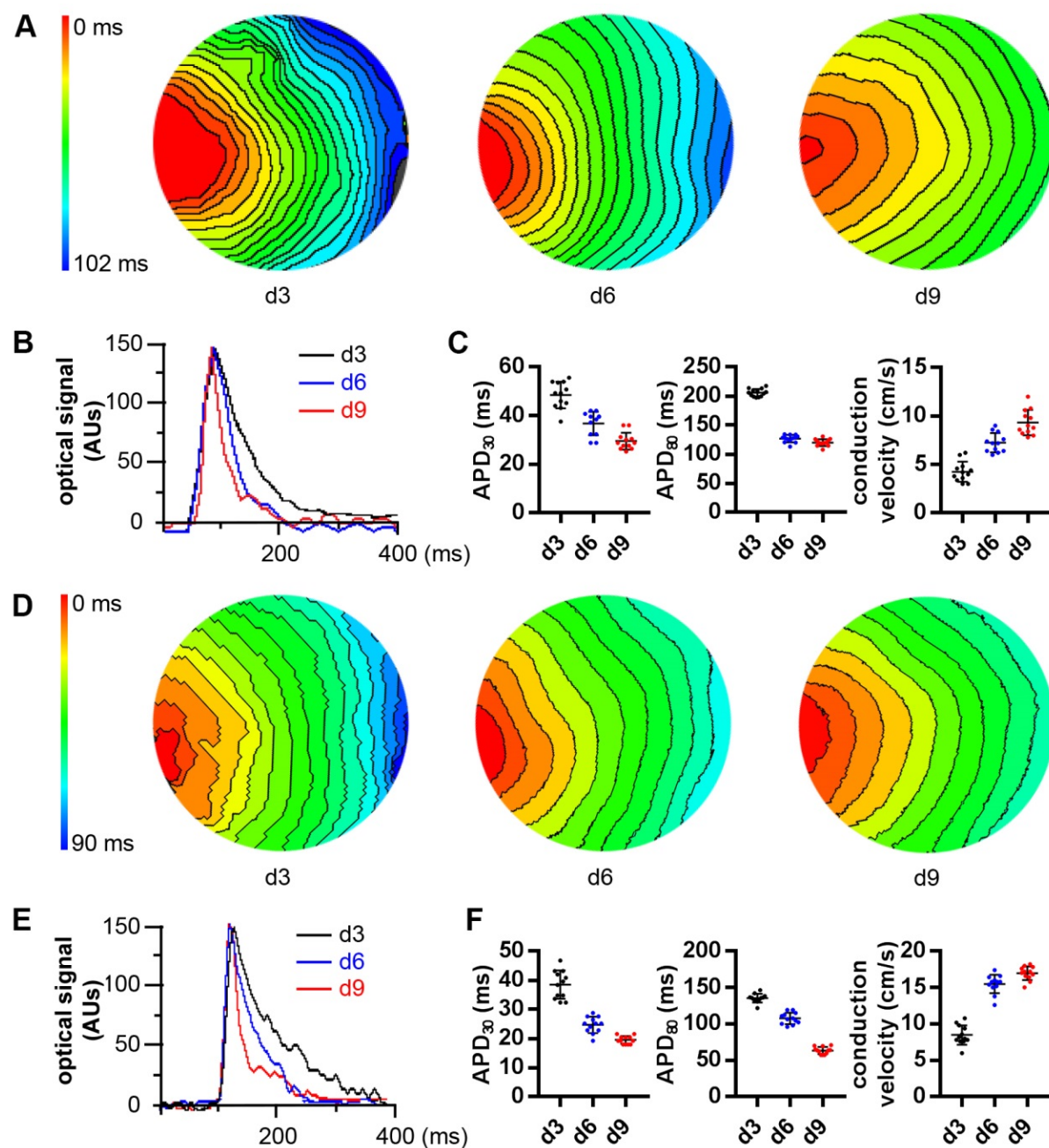


Figure S7. Characterization by optical voltage mapping and 1-Hz electrical point stimulation of confluent monolayers of iAM clones #1 (A-C) and #6 (D-F). Typical activation maps (A, D; isochrones are separated by 6 ms) and optical signal traces (B, E) acquired at different days after dox removal showing an increase in CV and a decrease in APD with advancing iAM differentiation. (C, F) Quantification of CV, APD₃₀ and APD₈₀ at 3, 6 and 9 days of iAM differentiation. Data are presented as mean±SD, N=12 cell cultures per group from 3 individual preparations. AUs, arbitrary units.

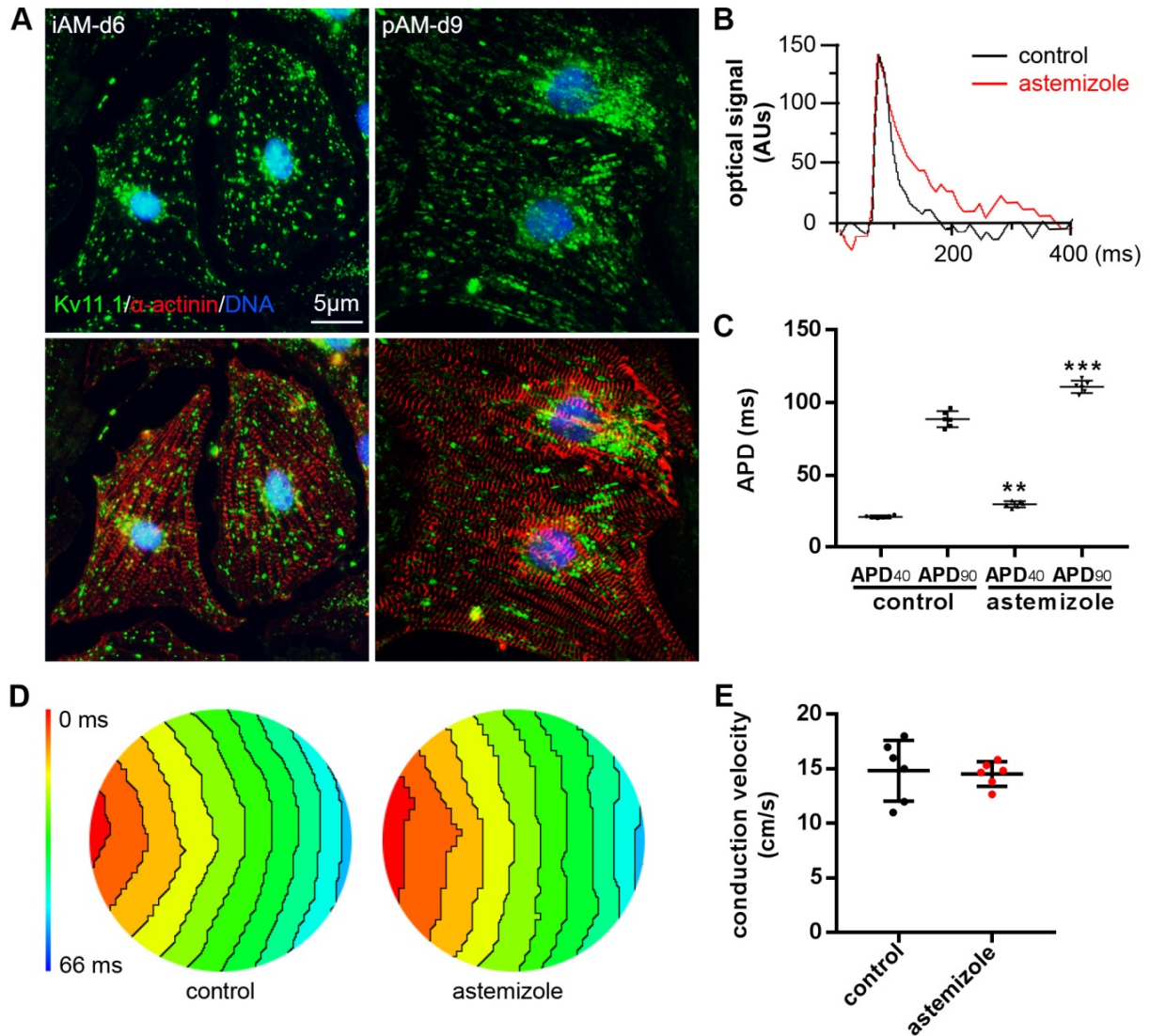


Figure S8. Suitability of iAMs as *in vitro* model to assess the I_{Kr} -blocking potential of drugs by optical voltage mapping. (A) Immunofluorescence analysis of $K_v11.1$ protein expression in iAM-d6 cultures and in 9-day-old pAM cultures. (B-E) Optical signal traces (B), quantitative analyses of APD₄₀ and APD₉₀ (C), activation maps (D) and CV (E) following 1-Hz pacing of iAM-d6 cultures exposed for 30 minutes to 100 nM astemizole or vehicle (control). Data are presented as mean \pm SD, N=6 cell cultures per group from 3 individual preparations. For statistical analysis, the nested ANOVA test was used. AUs, arbitrary units. ** P <0.01 vs control cultures.

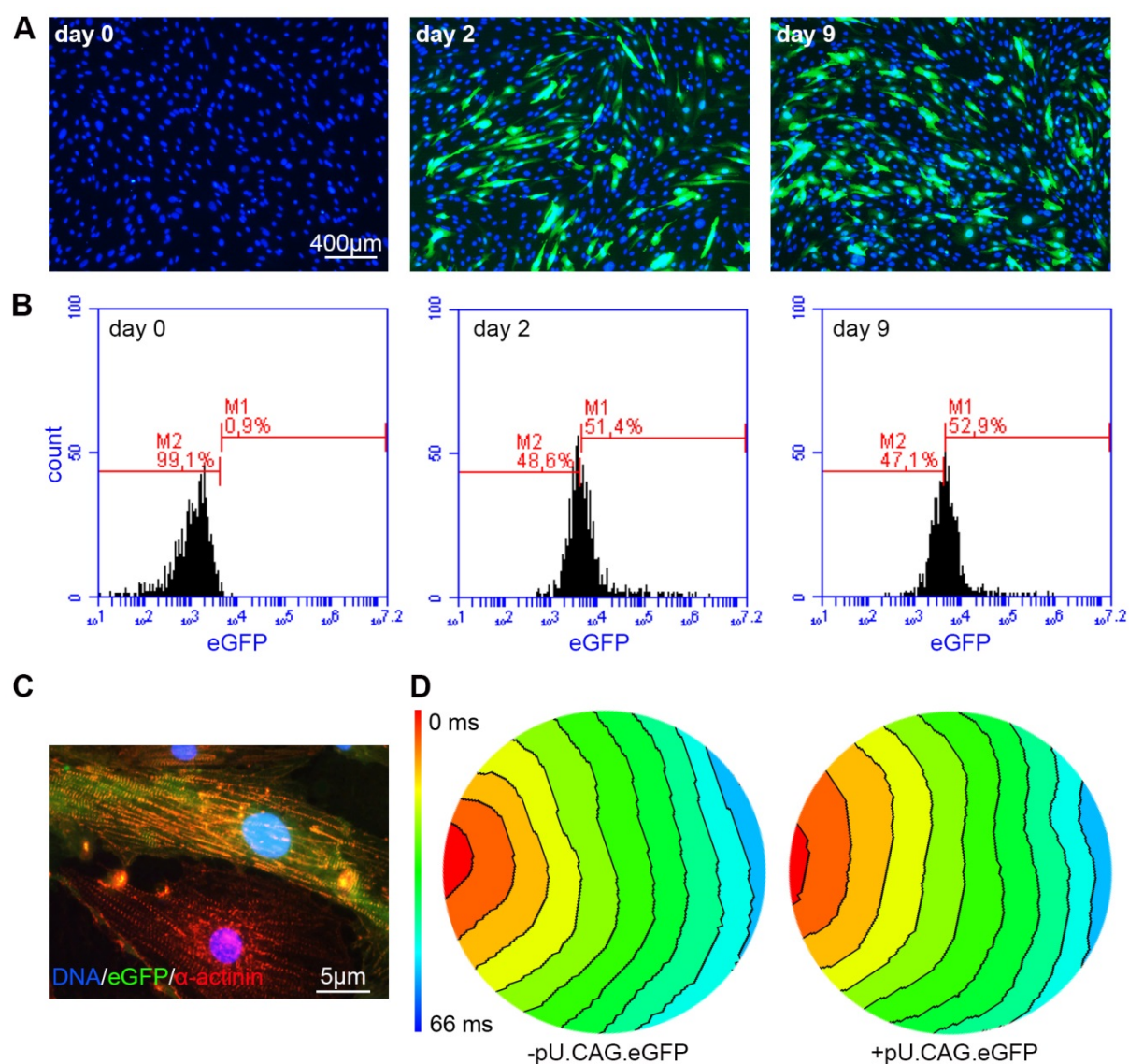


Figure S9. Transient transfection of iAMs with plasmid DNA. (A) Direct fluorescent images of iAMs immediately prior to lipofection (day 0) with the eGFP-encoding mammalian expression plasmid pU.CAG.eGFP (left panel) and following maintenance, after transfection, for 2 or 9 days in culture medium without dox (middle and right panel, respectively). (B) Quantification, by flow cytometry, of the percentage of eGFP⁺ cells in the cultures shown in (A). (C) Fluoromicrograph of an iAM culture that was transfected with pU.CAG.eGFP, subsequently maintained for 9 days in dox-free culture medium and finally immunostained for sarcomeric α -actinin. (D) Activation maps (6-ms isochrone spacing) of untransfected (-pU.CAG.eGFP) and pU.CAG.eGFP-transfected (+pU.CAG.eGFP) iAM cultures kept for 9 days in dox-free culture medium.

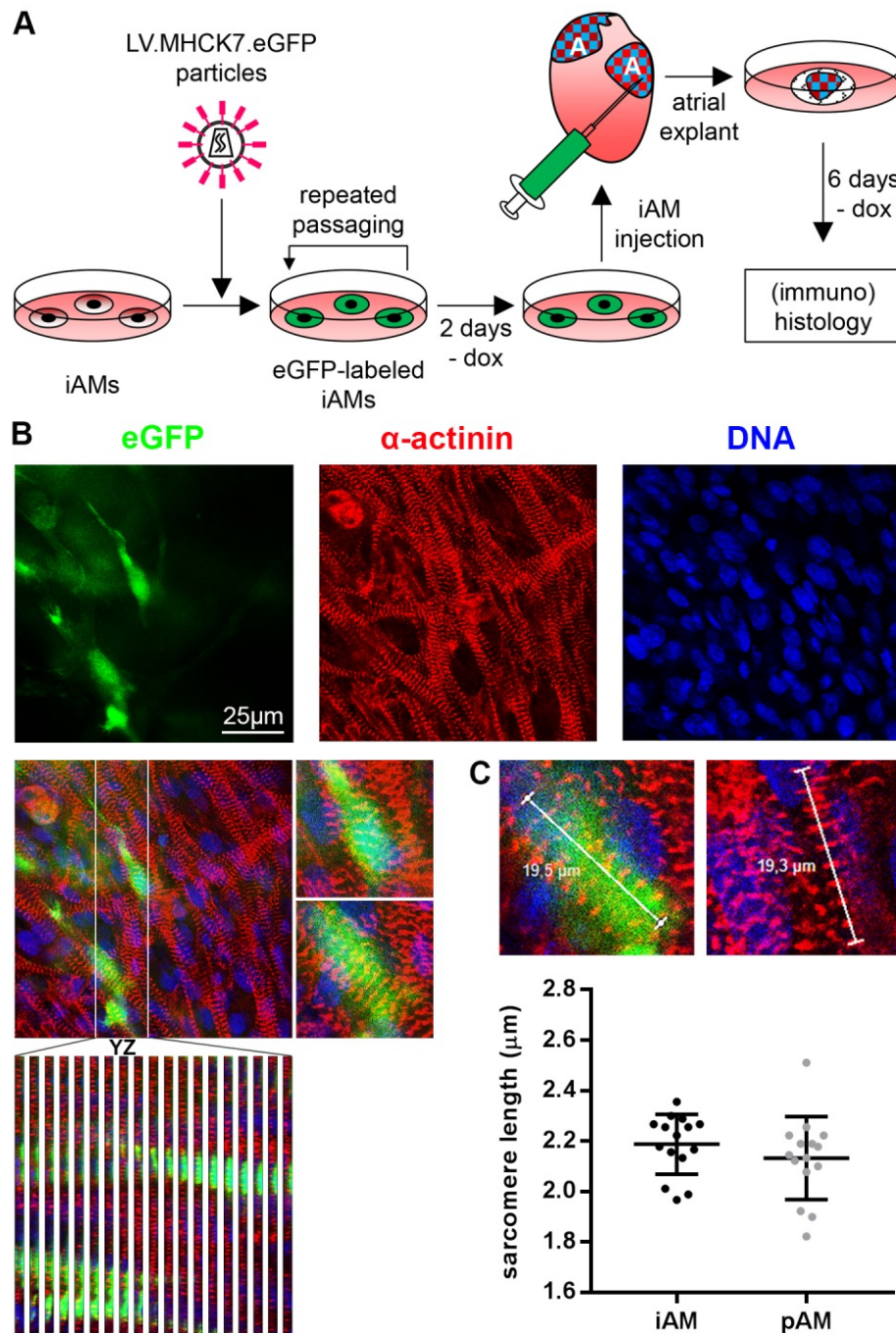


Figure S10. Structural integration of iAMs into neonatal rat atrium. (A) Experimental design to assess the engraftment and cardiomyogenic differentiation potential of iAMs following their injection into neonatal rat atrium. A, atrium. (B) Analysis by confocal laser scanning fluorescence microscopy of the presence and phenotype of eGFP-labelled iAMs following double immunostaining for eGFP (green) and sarcomeric α -actinin (red) and labelling of cell nuclei with Hoechst 33342 (blue). The 2 small panels in the middle row represent higher magnifications of the upper 2 eGFP⁺ cells in the adjacent larger panel. A series of YZ reconstructions of the eGFP⁺ cell-rich zone in this panel (area demarcated by white lines) is shown in the bottom panel. (C) Sarcomere lengths of endogenous pAMs and of iAMs that underwent cardiomyogenic differentiation following intra-atrial injection. Data are presented as mean \pm SD, N=15 cells per experimental group from 3 individual preparations. For statistical analysis, the nested ANOVA test was used.

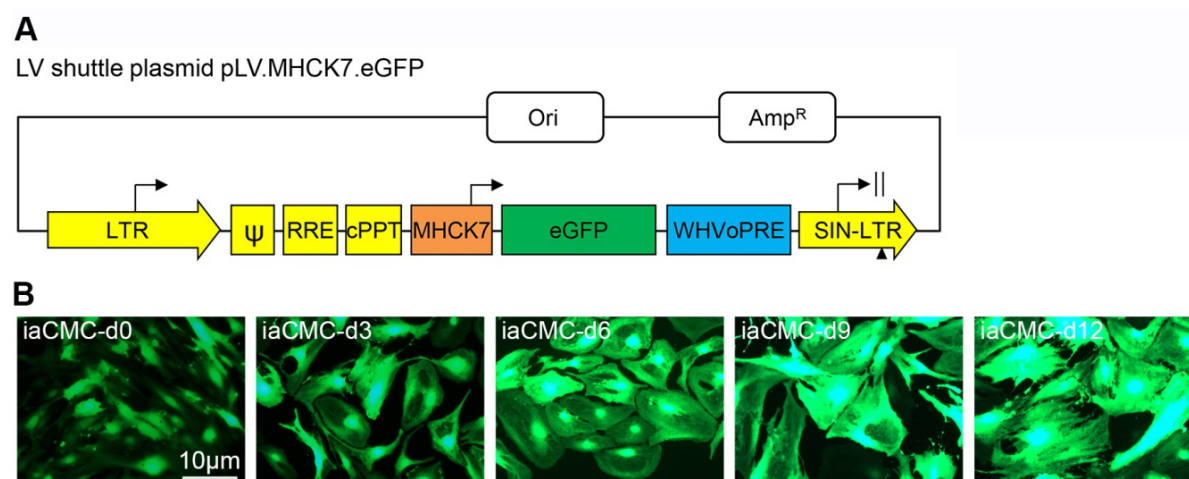


Figure S11. Activity of the MHCK7 promoter in proliferating iAMs and in iAMs at different days after initiation of cardiomyogenic differentiation. (A) Map of LV shuttle plasmid pLV.MHCK7.eGFP eGFP, eGFP-coding sequence. WHVoPRE, optimized version of the WHVPRE⁶, SIN-LTR, 3' long terminal repeat containing a 400-bp deletion in unique region 3 rendering the corresponding LV self-inactivating¹⁷. For an explanation of the other abbreviations, see *Figure 1A*. (B) Fluoromicrographs of LV.MHCK7.eGFP-transduced iAMs showing an increase in MHCK7 promoter activity, as evinced by an increase in eGFP fluorescence, with advancing iAM differentiation.

Movies

Movie I. iAM culture at 6 days after dox removal showing spontaneously contracting cells.

Movie II. iAM culture at 9 days after dox removal showing rhythmic contractions evoked by 1-Hz electrical point stimulation.

Movie III. Optical voltage recordings showing spreading of action potentials in a 9-day-old pAM culture, iAM cultures at 3 and 9 days after dox removal and an HL-1 culture following 1-Hz electrical point stimulation. The movie is played at 1/8th of the normal speed.

Movie IV. iAM culture at 9 days after dox removal showing reentrant conduction provoked by high-frequency electrical point stimulation. The movie is played at 1/8th of the normal speed.

Movie V. Neonatal rat atrial tissue injected with eGFP-labelled iAMs and kept in culture for 6 days showing spontaneous contractions.

Supplemental discussion

For most parenchymal cell types including cardiomyocytes, proliferation and (terminal) differentiation are mutually exclusive processes. Permanent LT expression, as occurs in the AT-1¹⁸, HL-1¹⁹ and AC²⁰ lines therefore does not allow the generation of homogeneous populations of differentiated cells. For HL-1 cells, this problem was partially overcome by culturing them in a highly specialized medium promoting their cardiomyogenic differentiation²¹. In order to control LT activity, Jahn *et al.*²² and Goldman *et al.*²³ relied on a temperature-sensitive version of the LT antigen (*i.e.* LT mutant *tsA58*) to immortalize neonatal rat and human foetal cardiomyocytes, respectively. Culturing of the neonatal rat cardiomyocytes at the non-permissive temperature of 39°C promoted their cardiomyogenic differentiation but still didn't yield excitable cells with well-developed sarcomeres whereas the human foetal cardiomyocytes failed to express cardiac differentiation markers at both the restrictive and permissive temperature. As an alternative method to control LT activity, Rybkin *et al.* generated transgenic mice containing an LT expression cassette under the control of cardiac-specific transcriptional regulatory elements of the murine *Nkx2.5* gene from which the LT-coding sequence could be excised using Cre recombinase. Cells isolated from the subendocardial tumor-like structures in the hearts of these animals could be serially passaged >50 times without showing obvious signs of senescence. Following removal of the LT-coding sequence by transduction with an adenovirus vector expressing Cre recombinase, the cells developed sarcomeres and some of them produced weak and slow Ca²⁺ transients after electrical stimulation. This, however, only occurred in low-serum medium containing insulin, transferrin and selenium or after ectopic expression of cardiomyogenic factors and did not result in the generation of contractile cells. Zhang *et al.*²⁴ also relied on the Cre-LoxP site-specific recombination system to generate lines of conditionally immortalized pVMs. Cre-mediated removal of the LT expression module and exposure to cardiomyogenic differentiation conditions did, however, not give rise to excitable or contractile cells.

The aforementioned immortalization strategy in which the immortalization gene is flanked with recombinase recognition sites to allow its excision following cell amplification thereby facilitating redifferentiation of the cells has some inherent disadvantages. Firstly, immortalization and subsequent deimmortalization of the cells requires two consecutive genetic manipulations. Secondly, due to the specific nature of the recombinase-mediated excision reaction, repeated switching between proliferative and differentiated cell states is impractical making deimmortalization essentially an irreversible process. Thirdly, recombinase-mediated excision reactions are never complete. Consequently, after recombinase treatment of a cell population there will always be a small fraction of cells that have retained the immortalization gene. As these cells will have a proliferative advantage, they will gradually “overgrow” the deimmortalized cells in the culture.

These drawbacks and the poor cardiomyogenic differentiation capacity of the deimmortalized cardiac muscle cell lines generated by Rybkin *et al.*²⁵ and Zhang *et al.*²⁴ prompted us to test another conditional immortalization strategy in an attempt to generate (fully) differentiation-competent cardiomyocyte lines. By transducing pAMs with an LV directing myocyte-selective and dox-dependent expression of the SV40

LT antigen, we succeeded to establish lines of cardiomyocytes showing rapid expansion in the presence of dox, while in its absence, the cells spontaneously and synchronously differentiated into fully functional (*i.e.* excitable and contractile) AMs.

As primary cultures of pAMs inevitably contain some non-cardiomyocytes (mainly cardiac fibroblasts), the myocyte-specific MHCK7 promoter^{4,5} was chosen to drive LT expression to avoid the fortuitous generation of non-cardiomyocyte clones. The success of this strategy critically depended on the MHCK7 promoter remaining active following the dedifferentiation of the AMs. Comparison of MHCK7 promoter activity in proliferating and differentiating AMs (*Figure S11*) showed that this was indeed the case. Cardiomyogenic differentiation led to an increase in the transcriptional activity of this promoter, consistent with the upregulation of cardiac transcription factor gene expression (*Figure 3A*). Nonetheless, LT expression was not detectable in differentiated iAMs either by western blotting or by IFM (*Figure 1C-E*). Concordantly, expression of the proliferation marker Ki-67 quickly ceased in the absence of dox (*Figure 2B and F*) indicating that soon after dox removal LT levels became too low to stimulate cell division.

Table S1 Primer pairs used for gene expression analysis

Gene	Forward primer	Reverse primer
<i>Actn2</i>	GGCTATGAGGAATGGCTATTGA	AAGTAGGGCTCGAACTTCC
<i>Atp2a2</i>	TGACCCACGAGCTGTTAATC	GGTGTTCCTCCTGTTCTGT
<i>Cacna1c</i>	CAAGGTGGTACACGAAGCTCA	ACAGTGCTGCCCTGGAGTA
<i>Gata4</i>	GGCTCTCTGGGAAACTGG	GAGGTGCCTAGTCCTTGC
<i>Kcnd3</i>	CAACTTTAGCAGGATCTACCATC	AGAGCTTCATTGAGGAGTCCA
<i>Kcnh2</i>	TAGCCTCCTCAACATCCC	CCATGTCTGCACTTAGCC
<i>Kcnj2</i>	GGATCTTACATGCTTCTGTAACC	CAGAGAACTTGTCCTGTTGC
<i>Kcnj3</i>	ACAGCCACATGGTCTCC	CCAGTTCAAGTTGGTCAAGG
<i>Kcnj5</i>	GGTTGTGGTCATACTAGAAGGG	GCAGTCATATCTGCCTTGGG
<i>Kcnj11</i>	GGAAGACCCGGAGGTAATAAG	CTCCACTCAGCTATCCTTCAC
<i>Mef2c</i>	GATTCAGATCACGAGGATTATGG	GTGCTGTTGAAGATGATCAGG
<i>Myh6</i>	CTACCAGATCCTGTCCAACAA	GCACATCAAAGGCGCTATC
<i>Myh7</i>	CACCAAGAGGGTCATCCAATA	CCAAATCGGGAGGAGTTATCA
<i>Myl2</i>	TTTGAGCAGACCCAGATCC	ACGTGTCCCTTAGGTCATTC
<i>Myl3</i>	GCTCTGGGACAGAATCCTAC	TCTTGGAGTTGAGCTCTTCC
<i>Myl4</i>	TCAGGGACTCTGCCTTTG	CCTCTTTGAATTCTTCGATCTGG
<i>Myl7</i>	TCAATGTTCGAGCAAGCC	CTGACTTGCAGATGATTCCG
<i>Nkx2.5</i>	CTCCCACCTTTAGGAGAAGG	CGAGGCATCAGGTTAGGTC
<i>Nppa</i>	CCAAGGGCTTCTTCCTCTTC	CTCATCTTCTACCGGCATCTTC
<i>Rn18s</i>	GTAACCCGTTGAACCCCATC	CCATCCAATCGGTAGTAGCG
<i>Ryr2</i>	AACTGGCCTTTGATGTTGGC	AATATGAGGTCGTCTCCAACCC
<i>Scn5a</i>	CCATTGTGCCCTGACGAACCTTA	GCTGCCTCCAGCTTCCACACA

Table S2 Antibodies

Antigen	Host	Dilution	Supplier	Catalogue number
LT	mouse	1:2,000 (WB) 1:200 (IC)	Santa Cruz Biotechnology	sc-147
GAPDH	mouse	1:100,000 (WB)	Millipore	MAB374
Ki-67	rabbit	1:200 (IC)	Abcam	Ab15580
Sarcomeric α -actinin	mouse	1:200 (IC)	Sigma-Aldrich	A7811
MLC2a	rabbit	1:200 (IC)	Non-commercial source	
Cx43	rabbit	1:200 (IC)	Sigma-Aldrich	C6219
K _v 11.1	rabbit	1:200 (IC)	Millipore	AB5930
eGFP	rabbit	1:200 (IC)	Thermo Fisher Scientific	A11122
Antigen	Host		Supplier	Conjugate
Mouse IgG	goat	1:15,000 (WB)	Santa Cruz Biotechnology	Horseradish peroxidase
Rabbit IgG (H+L)	donkey	1:400 (IC)	Thermo Fisher Scientific	Alexa 488
Mouse IgG (H+L)	donkey	1:400 (IC)	Thermo Fisher Scientific	Alexa 568

WB, western blotting; IC, immunocytochemistry.

Table S3 AP properties of pAMs and iAMs

	pAM (N=13)	iAM (N=15)
Upstroke velocity (mV/ms)	19.1±1.9	11.4±1.2**
AP amplitude (mV)	108.3±4.0	94.4±2.3
Overshoot (mV)	23.8±3.7	13.9±2.4*
APD ₃₀ (ms)	20.5±2.6	19.5±1.3
APD ₈₀ (ms)	74.2±9.5	70.0±6.9

Data represent mean±standard error of the mean (SEM). Statistical analysis was done using the nested ANOVA test. * $P < 0.05$; ** $P < 0.01$

Supplemental references

1. Loeber G, Tevethia MJ, Schwedes JF, Tegtmeyer P. Temperature-sensitive mutants identify crucial structural regions of simian virus 40 large T antigen. *J Virol* 1989;**63**:4426-4430.
2. Dinsart C, Cornelis JJ, Klein B, van der Eb AJ, Rommelaere J. Transfection with extracellularly UV-damaged DNA induces human and rat cells to express a mutator phenotype towards parvovirus H-1. *Mol Cell Biol* 1984;**4**:324-328.
3. Szulc J, Wiznerowicz M, Sauvain MO, Trono D, Aebischer P. A versatile tool for conditional gene expression and knockdown. *Nat Methods* 2006;**3**:109-116.
4. Salva MZ, Himeda CL, Tai PW, Nishiuchi E, Gregorevic P, Allen JM, Finn EE, Nguyen QG, Blankinship MJ, Meuse L, Chamberlain JS, Hauschka SD. Design of tissue-specific regulatory cassettes for high-level rAAV-mediated expression in skeletal and cardiac muscle. *Mol Ther* 2007;**15**:320-329.
5. Bingen BO, Engels MC, Schaliij MJ, Jangsangthong W, Neshati Z, Feola I, Ypey DL, Askar SF, Panfilov AV, Pijnappels DA, de Vries AA. Light-induced termination of spiral wave arrhythmias by optogenetic engineering of atrial cardiomyocytes. *Cardiovasc Res* 2014;**104**:194-205.
6. Schambach A, Bohne J, Baum C, Hermann FG, Egerer L, von Laer D, Giroglou T. Woodchuck hepatitis virus post-transcriptional regulatory element deleted from X protein and promoter sequences enhances retroviral vector titer and expression. *Gene Ther* 2006;**13**:641-645.
7. Feola I, Teplenin A, de Vries AA, Pijnappels DA. Optogenetic engineering of atrial cardiomyocytes. *Methods Mol Biol* 2016;**1408**:319-331.
8. Ramkisoensing AA, De Vries AA, Schaliij MJ, Atsma DE, Pijnappels DA. Brief report: Misinterpretation of coculture differentiation experiments by unintended labeling of cardiomyocytes through secondary transduction: delusions and solutions. *Stem Cells* 2012;**30**:2830-2834.
9. Majumder R, Engels MC, de Vries AA, Panfilov AV, Pijnappels DA. Islands of spatially discordant APD alternans underlie arrhythmogenesis by promoting electrotonic dyssynchrony in models of fibrotic rat ventricular myocardium. *Sci Rep* 2016;**6**:24334.
10. Yu Z, Liu J, van Veldhoven JP, AP IJ, Schaliij MJ, Pijnappels DA, Heitman LH, de Vries AA. Allosteric modulation of Kv11.1 (hERG) channels protects against drug-induced ventricular arrhythmias. *Circ Arrhythm Electrophysiol* 2016;**9**:e003439.
11. Kubalak SW, Miller-Hance WC, O'Brien TX, Dyson E, Chien KR. Chamber specification of atrial myosin light chain-2 expression precedes septation during murine cardiogenesis. *J Biol Chem* 1994;**269**:16961-16970.
12. Tristani-Firouzi M, Chen J, Mitcheson JS, Sanguinetti MC. Molecular biology of K⁺ channels and their role in cardiac arrhythmias. *Am J Med* 2001;**110**:50-59.
13. Ramos-Mondragón R, Vega AV, Avila G. Long-term modulation of Na⁺ and K⁺ channels by TGF-β1 in neonatal rat cardiac myocytes. *Pflugers Arch* 2011;**461**:235-247.
14. Wilson JR, Clark RB, Banderali U, Giles WR. Measurement of the membrane

- potential in small cells using patch clamp methods. *Channels* 2011;**5**:530-537.
15. Kannankeril P, Roden DM, Darbar D. Drug-induced long QT syndrome. *Pharmacol Rev* 2010;**62**:760-781.
 16. Delpon E, Valenzuela C, Tamargo J. Blockade of cardiac potassium and other channels by antihistamines. *Drug Saf* 1999;**21 Suppl 1**:11-18; discussion 81-17.
 17. Zufferey R, Dull T, Mandel RJ, Bukovsky A, Quiroz D, Naldini L, Trono D. Self-inactivating lentivirus vector for safe and efficient in vivo gene delivery. *J Virol* 1998;**72**:9873-9880.
 18. Steinhilber ME, Cochrane KL, Field LJ. Hypotension in transgenic mice expressing atrial natriuretic factor fusion genes. *Hypertension* 1990;**16**:301-307.
 19. Claycomb WC, Lanson NA, Jr., Stallworth BS, Egeland DB, Delcarpio JB, Bahinski A, Izzo NJ, Jr. HL-1 cells: a cardiac muscle cell line that contracts and retains phenotypic characteristics of the adult cardiomyocyte. *Proc Natl Acad Sci U S A* 1998;**95**:2979-2984.
 20. Davidson MM, Nesti C, Palenzuela L, Walker WF, Hernandez E, Protas L, Hirano M, Isaac ND. Novel cell lines derived from adult human ventricular cardiomyocytes. *J Mol Cell Cardiol* 2005;**39**:133-147.
 21. White SM, Constantin PE, Claycomb WC. Cardiac physiology at the cellular level: use of cultured HL-1 cardiomyocytes for studies of cardiac muscle cell structure and function. *Am J Physiol Heart Circ Physiol* 2004;**286**:H823-829.
 22. Jahn L, Sadoshima J, Greene A, Parker C, Morgan KG, Izumo S. Conditional differentiation of heart- and smooth muscle-derived cells transformed by a temperature-sensitive mutant of SV40 T antigen. *J Cell Sci* 1996;**109 (Pt 2)**:397-407.
 23. Goldman BI, Amin KM, Kubo H, Singhal A, Wurzel J. Human myocardial cell lines generated with SV40 temperature-sensitive mutant tsA58. *In Vitro Cell Dev Biol Anim* 2006;**42**:324-331.
 24. Zhang Y, Nuglozeh E, Toure F, Schmidt AM, Vunjak-Novakovic G. Controllable expansion of primary cardiomyocytes by reversible immortalization. *Hum Gene Ther* 2009;**20**:1687-1696.
 25. Rybkin II, Markham DW, Yan Z, Bassel-Duby R, Williams RS, Olson EN. Conditional expression of SV40 T-antigen in mouse cardiomyocytes facilitates an inducible switch from proliferation to differentiation. *J Biol Chem* 2003;**278**:15927-15934.